Reactivation of the p53 pathway by MDM2 inhibitor Nutlin-3: Application in photochemical internalisation (PCI)

Camilla Lavoll

Master's thesis at the

School of Pharmacy

Faculty of Mathematics and Natural Sciences

UNIVERSITY OF OSLO

May 2013

For the degree *Master of Pharmacy* (45 credits):

Reactivation of the p53 pathway by MDM2 inhibitor Nutlin-3: Application in photochemical internalisation (PCI)

Author

Camilla Lavoll

Main supervisor

Kristian Berg

Co-supervisor

Anette Weyergang

Department of Radiation Biology

Institute for Cancer Research

The Norwegian Radium Hospital

OSLO UNIVERSITY HOSPITAL

Department of Pharmacy

School of Pharmacy

Faculty of Mathematics and Natural Sciences

UNIVERSITY OF OSLO

UiO : School of Pharmacy
University of Oslo

2013

Reactivation of the p53 pathway by MDM2 inhibitor Nutlin-3: Application in photochemical internalisation (PCI)

Camilla Lavoll

http://www.duo.uio.no

Print: Reprosentralen, University of Oslo, Oslo, Norway

Abstract

With approximately 50% of tumours bearing mutations in the TP53 gene, the tumour suppressor p53 is one of the most frequently altered proteins in human cancer. In tumours retaining wild-type p53, other aberrations including overexpression of MDM2 may impair the function of the p53 pathway. MDM2 regulates p53 by inhibiting p53-mediated transcriptional activity and promoting its degradation. Inhibiting the MDM2-p53 interaction with small molecule antagonist Nutlin-3 is an attractive approach to reactivate p53 in tumours overexpressing MDM2. Photochemical internalisation (PCI) is a novel technology for the release of therapeutic macromolecules into the cytosol. The technology is based on the use of photosensitizers located in endocytic vesicles that upon activation by light induces release of the endocytosed macromolecules. In the current study, the $p53^{Wt}$ $MDM2^{Ampl}$ osteosarcoma cell line SJSA-1 was treated with a combination of Nutlin-3 and PCI of bleomycin or saporin to study the impact of Nutlin-3 on the p53 pathway. Treatment with PCI of bleomycin and Nutlin-3 resulted in increased expression of p53 and the p53 target genes MDM2, p21 and Bax. PCI of bleomycin in combination with Nutlin-3 also induced cell cycle arrest in the G_1/S checkpoint, but did not have a substantial impact on the induction of apoptosis. PCI of bleomycin and saporin both in presence and absence of Nutlin-3 inhibited cell growth, but the differences were negligible. These results indicate that Nutlin-3 in the concentration given in this study activates p53 leading to cell cycle arrest, while the effect on apoptosis remain ambiguous. The current study suggests that inhibition of the p53-MDM2 interaction with Nutlin-3 may be a promising strategy for improving tumour response to PCI in $MDM2^{Ampl}$ malignancies retaining wild-type p53.

Acknowledgements

The work in this thesis was carried out at the Department of Radiation Biology at the Institute of Cancer Research, Oslo University Hospital in the period of August 2012 to May 2013. It is the final part of a Master of Pharmacy at the School of Pharmacy, University of Oslo, and a number of people have helped me in this work.

Firstly, I would like to thank my main supervisor Professor Kristian Berg for this interesting project, for his invaluable inputs, for always being available for questions and discussions and for a very good balance of freedom and close follow-up. I would also like to thank my co-supervisor dr. Anette Weyergang for help with planning experiments, for supervision of work in the laboratory and for all your valuable comments.

Even if the words 'thank you' are in no way sufficient, I would like to thank Cathrine Elisabeth Olsen for all the help she has given me this year. Thank you for help with laboratory procedures, interpreting results, planning experiments and for all the great discussions we had this year. You were always helpful, positive, interested and approachable, and your contributions were invaluable.

I would like to thank the whole PCI group for letting me be part of a great work environment these past months. Thank you for all your inputs, help with laboratory work and for all the discussions, both serious and not so very serious.

Thank you to Marianne, Jagdip, Lise, Sissel and Trine, my fellow master students at the Department of Radiation Biology. We have had constructive discussions, encouraging chats, stressful times and a lot of fun this year, and I have sincerely enjoyed your company.

Finally, I want to thank my family and friends for all the support they have given me this year, and for making me take some time of when I needed it. It has been of great help.

Oslo, May 2013

Camilla Lavoll

Contents

Abbreviations

Ampl	Amplified
APS	Ammonium persulfate
Bax	Bcl-2-associated X protein
BLM	Bleomycin
BSA	Bovine serum albumin
Cdk	Cyclin-dependent kinase
CKI	Cyclin-dependent kinase inhibitor
ddH_2O	Double distilled water
dH_2O	Distilled water
DMSO	Dimethyl sulfoxide
DNA	Deoxyribonucleic acid
DTT	Dithiotreitol
EDTA	Ethylenediaminetetraacetic acid
FBS	Fetal bovine serum
IC	Internal conversion
ISC	Intersystem crossing
LD	Lethal dose
MDM2	Murine double minute 2
MTT	3-[4,5-dimethylthiazol-2-yl]-2,5-diphenyl tetrazolium bromide
Mut	Mutated
MW	Molecular weight
NT	No treatment
OD	Optical density
OSA	Osteosarcoma
PBS	Phosphate buffered saline
PDT	Photodynamic therapy
PCI	Photochemical internalization
PS	Photosensitizer
PVDF	Polyvinylidene difluoride
ROS	Reactive oxygen species
SDS	Sodium dodecyl sulfate

SDS-PAGE	Sodium dodecyl sulfate polyacrylamide gel electrophoresis
TdT	Terminal deoxynucleotidyl transferase
TEMED	Tetramethylethylenediamine
TP53	Tumour protein 53
$TPCS_{2a}$	Disulfonated tetraphenyl chlorine
$TPPS_{2a}$	Disulfonated tetraphenyl porphine
TUNEL	TdT-mediated dUTP Nick End Labeling
Wt	Wild-type
γH2AX	Phosphorylated Histone H2AX

Aim of the study

Despite many advances in cancer therapy there are still major challenges to overcome. Low specificity, dose-limiting toxicity and resistance to cytotoxic drugs are sources of therapeutic failure and severe side effects. New treatment regimes targeting tumours more specifically by exploiting their differences from normal cells hold great potential in cancer therapy.

Mutations of the tumour suppressor p53 are found in half of human malignancies, making the TP53 gene one of the most frequently mutated genes in cancer [1]. The remaining 50% of tumours express wild-type p53 and are thus capable of activating the p53 pathway. However, aberrations in p53 regulation or signalling may result in inadequate tumour suppression. One such aberration is amplification of MDM2, the negative regulator of p53 [2]. Mutation of p53 and MDM2 amplification is found to be largely independent making MDM2 an attractive target in tumours where non-functional p53 is due to overexpression of MDM2 protein [3].

The aim of this study was to investigate what impact the MDM2 inhibitor Nutlin-3 has on cell survival, cell cycle progression and expression of p53 and p53 downstream targets after PDT and PCI treatment in cell lines with different p53 and MDM2 status. The objective was to see if Nutlin-3 could increase efficacy of PCI treatment in tumours where p53 is non-functional due to MDM2 amplification.

1 Introduction

1.1 Background

The p53 gene is regarded as one of the most important genes in the development of human cancer [4]. Since its discovery more than 30 years ago, the tumour suppressor p53 has been subject of intense study yielding more than 60,000 PubMed-listed publications so far [5]. In 1994, Hollstein and colleagues revealed that approximately 50% of all human malignancies have mutations in the TP53 gene, making it one of the most frequently mutated genes in human cancer [6]. The tumour suppressor p53 is often called 'Guardian of the Genome' due to its role in preventing cells with irreparable DNA damage to proceed in the cell cycle. Several different types of DNA damage activate p53, resulting in a rapid increase in the p53 level in the cell and activation of p53 as a transcription factor [7]. This leads to a series of downstream events including cell cycle regulation and regulation of apoptosis, ultimately ensuring cellular and genetic stability [7].

In addition to mutations in the TP53 gene, p53 can be inactivated by other aberrations in the signalling pathway. One such aberration is amplification of the *Mdm2* gene or overexpression of the MDM2 protein. p53 and MDM2 form an autoregulatory feedback loop in which p53 positively regulates MDM2 levels and MDM2 negatively regulates p53 levels and activity [8]. In cells expressing wild-type p53 and normal levels of MDM2, various stress signals will lead to decrease in MDM2 protein levels and/or decrease in its interaction with p53, leading to p53 stabilization [9, 10]. In cells overexpressing MDM2, several studies have showed that p53 activity is attenuated, increasing the susceptibility for tumour formation [3]. A screening of more than 3000 tumours from 28 tumour types showed that of the tumours with mutation in either p53 or MDM2, only 4% showed mutations in both genes [3]. Therefore, antagonizing MDM2 to restore p53 function is a promising approach in cancer therapy. Different methods have been exploited to release p53 from MDM2 control including blocking MDM2 expression, inhibiting MDM2 ubiquitin ligase activity and inhibiting the MDM2-p53 binding [11]. Several classes of low molecular weight inhibitors of the p53-MDM2 interaction have been reported to disrupt the binding of the two proteins [12]. In 2004, Vassilev and colleagues at Roche Research Centre (Nutley, NJ, USA) discovered a series of *cis*-imidazoline analogues that can displace p53 from its complex with MDM2 [13].

The compounds were given the name Nutlins, and have shown the ability to activate the p53 pathway in vitro and in vivo in tumours expressing wild-type p53 [12].

1.2 The cell cycle

When DNA is damaged, for instance after irradiation or exposure to certain chemicals, it is crucial that this is repaired before the cells duplicate or segregate the chromosomes. Eukaryotic cells have evolved a complex network of regulatory proteins known as the cell cycle control system. This system monitors progression through the cell cycle and delays later events until earlier events have been completed. Preparations for the segregation of replicated chromosomes, for example, is inhibited until DNA replication is completed [14]. In this way, the cell will not proceed in the cell cycle with chromosomes that is either incompletely replicated or damaged, which can lead to development of cancer.

The cell cycles basic function is to duplicate the DNA in the chromosomes accurately and then segregate the copies precisely into two genetically identical daughter cells. This process is carried out in the two main phases of the cell cycle named S phase and M phase. In S phase the DNA duplication occurs with subsequent chromosome segregation and division in M phase. In addition to this there are two gap phases – G_1 phase between M phase and S phase and G_2 phase between S phase and M phase. These two gap phases allow time for growth and provide the cell with time to monitor the internal and external environment to ensure that everything is complete and that the conditions are suitable for the cell to enter the next phase [15].

At the end of each G-phase in the cell cycle, there is a checkpoint restricting the progression to the next phase. A family of protein kinases known as cyclin-dependent kinases (Cdks) govern these checkpoints, and the activity of these kinases fluctuates throughout the cell cycle. Their activity leads to cyclical changes in the phosphorylation of intracellular proteins that initiate or regulate the events in the cell cycle. The G_1/S-cyclins, for example, binds Cdk at the end of G_1 and commit the cell to DNA replication [16]. When the cell is exposed to radiation, chemicals or other potential harm, the cell-cycle control system detects the DNA damage and arrests the cell cycle at DNA checkpoints. Subsequently, DNA repair is induced, and upon completion the cell will continue in the cell cycle. In the event of irreparable damage, apoptosis is induced to ensure that a cell with DNA damage does not continue to replication or undergo mitosis [17]. The signals governing cell fate is largely

unclear, but the cell cycle checkpoint and signalling pathways inhibiting entry to S phase is known to be intimately associated with the tumour suppressor p53 [17, 18].

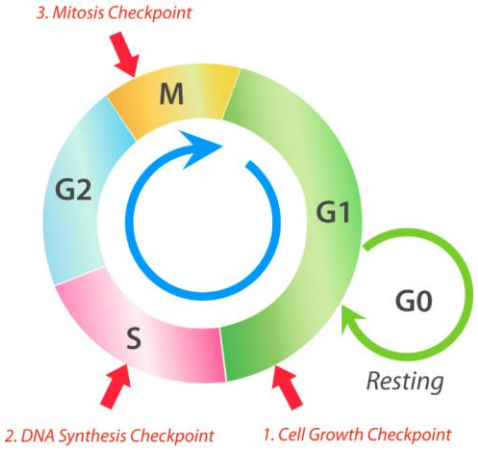

Figure 1.1: Illustration of the cell cycle in eukaryotic cells. At the checkpoints the status of the cell is controlled to make sure that the cell can continue to the next phase. If the cell at the G_1/S checkpoint is not ready to continue to S-phase, the cell can go through a resting period (G_0) until it is ready to divide. Adapted from Moodle.org [19]

1.3 p53

The biological role of p53 is as pointed out above to ensure genetic stability, and p53 is often referred to as the cell's gatekeeper because if its role in the G_1/S checkpoint. Upon DNA damage, p53 can stimulate the repair processes and protective mechanisms, or if necessary, the cessation of cell division and the induction of controlled cell death [17].

In proliferating cells, the p53 protein is kept at a low level, predominantly through MDM2-mediated ubiquitination and degradation [20]. p53 is a potent anti-proliferative and pro-apoptotic protein, and high levels can therefore harm normal cells [11]. Normally, p53 has a relatively short half-life of about 6-20 minutes, but when the degradation of the protein is inhibited following various forms of cellular stress, the half-life of p53 is lengthened to hours resulting in a 3-10-fold increase in p53-concentration in the cell [7, 21, 22]. Following p53 accumulation, the transcription of the gene encoding the cyclin-dependent kinase inhibitor (CKI) $p21^{Waf1}$ is stimulated [14]. p21 is capable of silencing the Cdks which are essential for S phase entry, and thereby activating the G_1/S checkpoint [18]. The checkpoint arrest following DNA damage has two potential impacts. It allows extra time for repair to take place before cell cycle progression, and it can permanently prevent proliferation in severely damaged cells [23]. Upon irreparable DNA damage, p53 can induce apoptosis

primarily through two distinct apoptotic signalling pathways. The extrinsic pathway involves engagement of particular 'death' receptors, leading to a cascade of activation of caspases, which in turn induce apoptosis [24]. The intrinsic pathway is associated with mitochondrial depolarization and release of cytochrome c from the mitochondrial intermembrane space into the cytoplasm leading to caspase activation. The intrinsic apoptotic pathway is dominated by the Bcl-2 family proteins including the pro-apoptotic protein Bax, which in response to stress activation forms a homodimer and releases cytochrome c from the mitochondria leading to caspase activation [24]. What determines if p53 induces cell cycle arrest or apoptosis upon DNA damage is only partially understood, and is subject of intense study.

1.3.1 Non-functional p53

In the early years of p53 research, the protein was mistakenly classified as an oncogene because high levels of p53 was detected in a number of tumour-derived cell-lines [5]. This perception was later challenged when it was revealed that the initially discovered p53 in fact was a mutant form of the protein. In sharp contrast to these mutant forms, wild-type p53 turned out to be capable of supressing the malignant growth of transformed cells [25]. Following this discovery, p53 have been subject to extensive research with the objective to reveal what makes p53 lose its tumour suppressor properties, and what can be done to circumvent this loss of function.

The function of the TP53 gene is usually altered through mutations, loss of hetrozygosity (LOH) or in a few cases through DNA methylation [26]. In over 50% of tumours, TP53 is inactivated due to loss of function mutations and around 95% of them are found within the genomic region encoding the sequence-specific DNA-binding domain of TP53. These mutations disrupt the proper confirmation if those sequences, making mutant forms of TP53 lose the sequence-specific transactivation ability [26]. Thus, loss in p53 activity alters the ability for DNA repair and may contribute to the development of cancer.

In some tumours with wild-type p53, other aberrations in the pathway such as the amplification of the *Mdm2* gene or overexpression of the MDM2 protein can block p53 function and promote growth of the tumour. Mutations in p53 and amplification of MDM2 have shown to be largely independent of each other, and might therefore present a different approach in the search for more effective treatment of tumours with wild-type p53 [3].

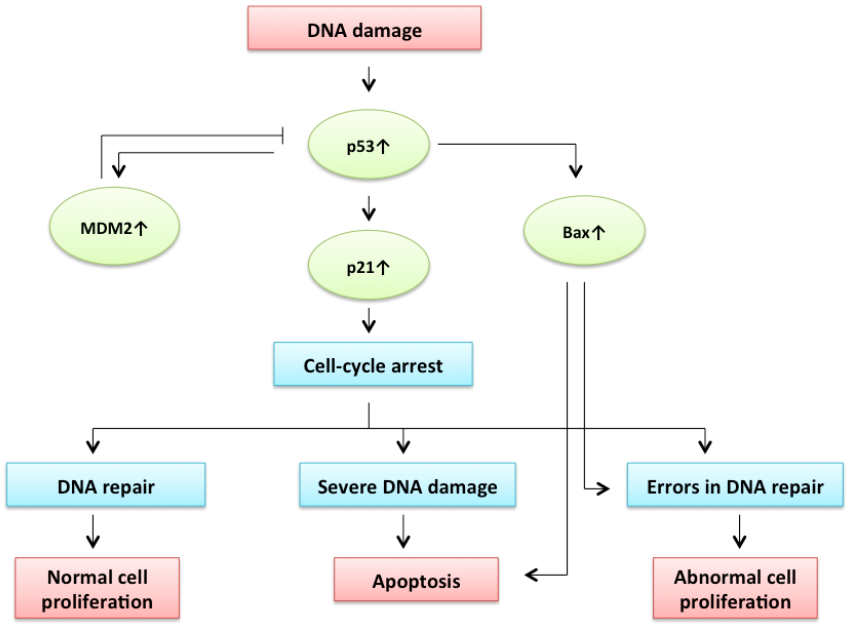

Figure 1.2: Schematic illustration of the activation of the p53 pathway following DNA damage. Adapted from Matsumura *et al.* 2002 [27]

1.4 Murine double minute 2 (MDM2)

As mentioned previously, the level of p53 is kept low by MDM2-mediated regulation and physical and functional interaction between the two proteins [9]. MDM2 functions mainly, if not exclusively as an E3 ligase, targeting p53 for ubiquitylation and thereby controlling the protein level by proteasome-dependent degradation. In addition to degrading p53, MDM2 can antagonize p53 by concealing its transactivation domain. This is done by binding to an N-terminal region of p53, thereby blocking its ability to associate with the transcriptional machinery [9].

In a normal unstressed cell, any increase in the p53 level will subsequently activate MDM2 that in turn targets p53 for degradation. In response to stress, a decrease in MDM2 protein levels and/or its activity and the interaction between MDM2 and p53 leads to p53 stabilisation and subsequently activation of the p53 pathway [9]. This reduction of MDM2 in response to stress is crucial for p53 to exert its tumour suppressor activity.

Around 50% of all tumours have non-functional p53 due to mutations, but the remaining 50% express wild-type p53 and are therefore capable of activating the p53 pathway. However, aberrations in p53 regulation and/or defective signalling in the p53 pathway is a frequent cause for inadequate tumour suppression [2]. One such aberration includes the murine double minute-2 gene product, MDM2. The MDM2 gene is found to be

abnormally upregulated in many human tumours including 13% of human esophageal carcinomas, 16% of osteogenic sarcomas and 20% of soft tissue sarcomas [2]. Amplification of MDM2 promotes cell growth, accelerates tumourigenesis and correlates with tumour incidence and clinical prognosis. Since p53 mutations and MDM2 amplification tend to be mutually exclusive events, reactivating p53 through antagonising MDM2 has been proposed as a new approach in treatment of tumour retaining wild-type p53 [2].

1.5 Inhibiting the p53-MDM2 interaction

Historically, it has been difficult to develop inhibitors of protein-protein interactions due to the large binding interface of the protein partners [28]. Protein interfaces are often large, flat and featureless, and frequently contain buried surfaces [2]. However, studies on the crystal structure of MDM2 revealed that the protein possesses a relatively deep hydrophobic cleft for p53 binding, with three amino acid residues contributing to a large part of the interaction and binding energy [2, 13]. To identify compounds that could inhibit the p53-MDM2 interaction, Vassilev *et al.* screened a diverse library of synthetic chemicals, identifying several promising compounds and optimised them for potency and selectivity [13]. One class of compounds that came out of this process was a series of *cis*-imidazoline analogues that was named Nutlins. These compounds displaced recombinant p53 protein from its complex with MDM2 with a mean inhibitory concentration (IC_{50}) values in the 100 to 300 nM range [13]. Three Nutlins, Nutlin-1, Nutlin-2 and Nutlin-3 all disrupt the p53-MDM2 interaction, but Nutlin-3 is the compound most extensively evaluated for its therapeutic potential and mechanism of action [28]. The compounds were made as a racemic mixture from which the enantiomers could be separated. Only one of the enantiomers, called enantiomer-a, possessed potent binding activity and it was 150 times more active than the other enantiomer, enantiomer-b [13]. The active enantiomer of Nutlin-3 was purified, and is now known as Nutlin-3a [12].

1.5.1 Nutlin-3

After its discovery almost 10 years ago, Nutlin-3 has been subject of extensive research. It has proven to be a potent and selective inhibitor of the p53-MDM2 interaction with excellent cell permeability. It induces accumulation and activation of p53 in cancer and normal cells without inducing DNA damage, thus being a non-genotoxic agent for the activation of p53

[28]. Proliferating cancer cells were effectively blocked in G_1 and G_2 phases, and underwent apoptosis when exposed to concentrations of Nutlin in the micromolar range [11].

Nutlin-3 has been studied in a vide variety of cell lines with different p53 and MDM2 status. Studies including cytotoxic drugs in combination with Nutlin-3 have shown improved response to chemotherapy in cell lines retaining wild-type p53 [1, 29-32]. Several studies investigating the differences in response to Nutlin-3 in $p53^{Wt}$ and $p53^{Mut}$ cell lines has shown that Nutlin-3 induces cell cycle arrest and apoptosis in cell lines with $p53^{Wt}$ and not in $p53^{Mut}$ [33-35].

While the efficiency of Nutlin-3 treatment of tumours with $MDM2^{Ampl}$ and $p53^{Wt}$ is confirmed in numerous studies, the response in cancer cells with normal levels of MDM2 is still unclear [1]. The apoptotic response of Nutlin-3 in these cell lines can vary dramatically, and future studies are necessary to investigate the utility of Nutlin-3 in cancer therapy. What tumour types that are particularly sensitive to inhibitors of the p53-MDM2 interaction, if treatments with these agents can lead to mutations in p53 or other defects in the p53 pathway and if the inhibitors can be used as monotherapy or in combination regimens in treatment of cancers with mutated p53, are amongst the other issues that needs to be addressed [28].

1.6 Photodynamic therapy (PDT)

1.6.1 Background

The use of light as a therapeutic agent can be traced back thousands of years. It was used in ancient Egypt, India and China in the treatment of skin diseases, such as psoriasis, vitiligo and cancer, as well as rickets and even psychosis. However, it is only relatively recently that light has been used to any significant degree in medicine [36]. Throughout the 20^{th} century, many great discoveries were made in the field of photodynamic therapy (PDT). In 1901, the Danish physician Niels Finsen described the successful treatment of small pox using red light. Later, he used ultraviolet light to treat cutaneous tuberculosis. Finsen was awarded the Nobel Price in 1903 for his work in phototherapy [36]. In the 1960s, Richard Lipson and colleagues initiated the modern era of PDT at the Mayo Clinic. Through experiments they demonstrated that a compound called ‘haematoporphyrin derivative’ (HDP) was a photosensitizing agent, and thus had the capability to capture radiant energy and shuttle it into a biological system [37].

The application of PDT in cancer therapy took a long time to develop. In 1972, Diamond *et al.* published results indicating the possible use of haematoporphyrin as a selective photosensitizing agent to destroy tumour cells by exposure to visible light [38]. A significant breakthrough came in 1975 when Dougherty and colleagues reported that exposure of rat and mouse tumours to red light after injection of haematoporphyrin resulted in a substantial number of long-term cures [39]. In the last part of the 20^{th} century, the field of photodynamic therapy expanded substantially, including human trials, many new photosensitizing agents and new clinical applications.

1.6.2 Principle

Photodynamic therapy consists of 3 components: a photosensitizer (PS), light and oxygen. Individually, none of these components are toxic, but when a photosensitizer is irradiated in the presence of oxygen, a highly reactive product named singlet oxygen ($^1O_2$) is generated [40]. Following the absorption of light, the sensitizer is excited from its ground state, p^0, to excited singlet stated, $^1p^*$. From here it can return to the ground state by emitting a fluorescent photon (fluorescence) or to triplet excited state, $^3p^*$, through intersystem crossing (ISC). From the triplet excited state, the sensitizer can return to the ground state by emitting a phosphorescent photon (phosphorescence), by internal conversion (IC) or by transferring energy to another molecule [41]. The latter can occur through two different reactions. It can transfer electrons (dominating) or hydrogen atoms directly to O_2 or to a substrate to form radicals that later can interact with oxygen to produce oxygenated products (type I reaction). The second option is energy transfer from the excited triplet directly to ground-state molecular oxygen ($^3O_2$) to form excited O_2, so called singlet oxygen ($^1O_2$) (type II reaction) [42]. Both type I and type II reactions may occur during treatment. Although type II reactions are reported to dominate during PDT [41], the ratio between the two reactions depend on the type of sensitizer used, the concentrations of substrate and oxygen and the binding affinity of the sensitizer for the substrate [42].

The half-life of singlet oxygen in biological systems has been reported to be less than 0,04 μs with a radius of action of less than 0,02 μm [43]. Consequently, only cells that are in close proximity to the accumulated photosensitizer, and thus the ROS generation, are directly affected by PDT [42]. The anti-tumour effects of PDT derive from 3 inter-related mechanisms. Direct cytotoxic effects on tumour cells are achieved by PDT generated ROS. The effectiveness of direct tumour-cell killing is dependent on the distribution of the

photosensitizer within the tumour and the availability of oxygen within the targeted tissue. Therefore, complete tumour eradication is not always possible with this mechanism alone. The second effect of PDT is damage to the tumour vasculature. PDT causes microvascular collapse, thus cutting off the tumours supply of nutrients and oxygen and thereby inducing cell death [42]. The last important anti-tumour effect of PDT is the induction of an inflammatory reaction which in turn can lead to the development of systemic immunity [40]. Reports indicate that, while the direct cytotoxic effects of PDT can destroy the bulk of the tumour, the immune response is required to eliminate the surviving cells. The relative importance of these 3 mechanisms is yet to be defined, but it is clear that a combination is necessary to ensure long-term tumour control [42].

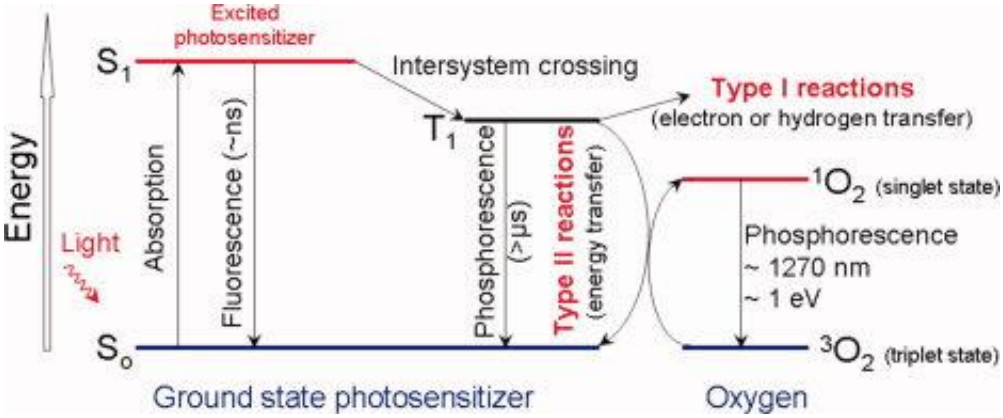

Figure 1.3: Photosensitisation processes illustrated by a modified Jablonski diagram. Upon light exposure the molecule is excited from a ground singlet state (S_0) to an excited singlet state (S_1). It may then undergo intersystem crossing to an excited triplet state (T_1) and then either form radicals via a Type I reaction or transfer its energy to molecular oxygen ($^3O_2$) and form singlet oxygen ($^1O_2$). Adapted from Agostinis *et al.* 2011 [40].

1.6.3 Photosensitizers

The ideal photosensitizer should meet several criteria: It should be a single pure compound to allow quality control with low manufacturing costs. Because the penetration of light into tissue increases with its wavelength, it should have a high absorption peak in the red to deep red area. It should have no dark toxicity and relatively rapid clearance from normal tissue, thereby minimalizing phototoxic side effects [40]. Some of the most useful photosensitizers for *in vivo* PDT are porphyrins, chlorins and bacteriochlorins [41]. Most of them are planar-aromatic molecules composed of four symmetrically arranged pyrrol units linked by methine

bridges. They all have a strong absorption band around 400 nm, but this is not clinically relevant due to the low tissue penetration of blue light [41].

The first photosensitizer to be used in the clinic was the mixture of phorpyrins called hematoporphyrin derivative (HPD), which later was released on the market in the purified form with the name Photofrin® [40]. Photofrin® is the most commonly used and studied photosensitizer, but due to some disadvantages, including long-lasting skin photosensitivity and a relatively weak absorption band at 630 nm, there is a need for better photosensitizers [40, 41]. In recent years, several new photosensitizers have been developed. Foscan® (temoporfin), Visudyne® (verteporfin), Levulan® (5-aminolevulinic acid) and the precursor Metvix® (methyl aminolevulinate) have all been approved for clinical use, and several promising photosensitizers are currently in clinical trials [44].

1.7 Photochemical internalisation (PCI)

1.7.1 Background

Macromolecules hold great potential in cancer therapy due to their prospects of higher therapeutic specificity than for most smaller molecular chemotherapeutic agents [45]. Macromolecules that are unable to pass directly through the cellular membrane because of their high molecular weight are therefore taken up into the cells by means of endocytosis [46, 47]. Endocytosis involves internalisation of extracellular substances through invagination of the cell membrane, resulting in an endocytic vesicle containing the substances [46]. These endocytic vesicles (endosomes) have several potential destinations, mainly the lysosomal compartment for degradation, or recycling back to the cell surface [48]. For the therapeutic macromolecules with intracellular targets to exert their activity, they need to be released from the endosomes and enter the cytosol before they are degraded by lysosomal enzymes [49].

1.7.2 Principle

Photochemical internalisation (PCI) is based on the same principles as photodynamic therapy (PDT), and share many of the same characteristics [46]. PCI is a novel technology for release of endocytosed macromolecules into the cytosol [50]. The technology is based on the use of photosensitizers that locate in endocytic vesicles, and that upon activation by light disrupts the endocytic vesicle, thereby facilitating the release of the macromolecules [46, 50]. When the photosensitizer is exposed to light, reactive oxygen species (ROS) form the same way as for PDT. The chemical reactions induced by ROS ruptures the membrane, and allow the

molecules to vacate the endosomes [46]. This photochemically induced release is shown to occur without inducing extensive cell death, and with maintenance of the biological activity of the released molecules [51]. As pointed out above, singlet oxygen $^1O_2$ has a very short lifetime and a short range of action, and may therefore destroy the membranes while the contents of the vesicles remain functionally intact [49]. Therapeutic agents for photochemical delivery include proteins toxins, oligonucleotids, nanoparticles and chemotherapeutic agents [46].

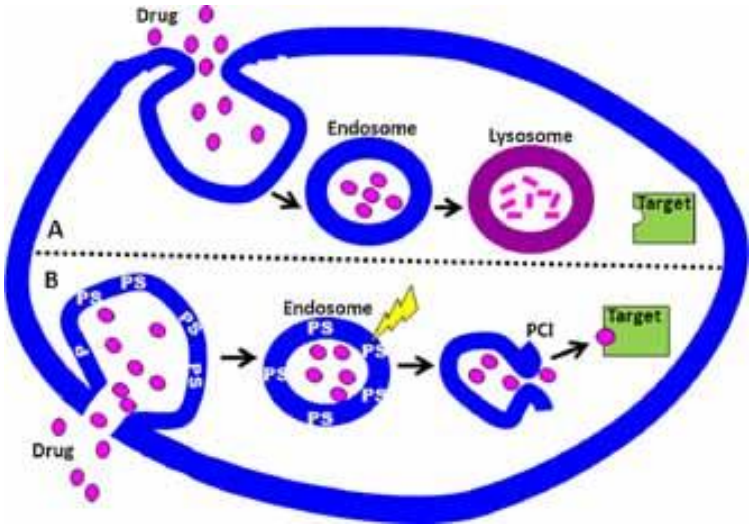

Figure 1.4: Schematic illustration of PCI. **A:** Drugs taken up through endocytosis are transported to endosomes where they are degraded before they have exerted their action. **B:** PCI is based on accumulation of photosensitizer (PS) in endosomes and lysosomes. Light exposure causes rupture of the endo/lysosomal membrane and releases the drug into the cytosol where it can exert its action. Adapted from Weyergang *et al.* 2011 [52].

1.7.3 Photosensitizers

For clinical use, the photosensitizers for PCI treatment should meet the same criteria as for PDT, considering toxicity, pharmacokinetics and light absorbance. In addition, photosensitizers used in PCI should have certain properties. They should localize in the endocytic vesicles. Within these vesicles, they should preferably localize to the membranes in order to give maximum damage to the membrane and minimum destruction of the internalized molecules. The aggregation of the photosensitizer within the cell should also be kept low, because aggregates reduce the ability of the photosensitizer to transfer the energy of the excited state to molecular oxygen [51]. The most efficient photosensitizers used in PCI have an amphiphilic structure with a hydrophilic part inhibiting penetration through cellular

membranes [46, 50]. The photosensitizer will intrude into the plasma membrane and enter the cells via endocytosis, ending up in the inner leaflet of the endocytic vesicles [46].

Over the last 20 years, several hundred new photosensitizers have been developed for use in PDT. The most promising or approved ones exert with a few exceptions amphiphilic properties, but their ability to penetrate cellular membranes makes them unsuitable for use in PCI [50]. Photosensitizers with two sulfonate-groups instead of carboxyl-groups cannot penetrate cellular membranes, and are therefore applicable for PCI. Sulfonate groups have low pK_a values, prohibiting protonation even in the acidic lysosomes [50].

The preclinical evaluation of PCI have been performed with the endosomally localized photosensitizers aluminium phtalocyanine disulfonate ($AlPcS_{2a}$), disulfonated tetraphenyl porphine ($TPPS_{2a}$) and disulphonated tetraphenyl chlorin ($TPCS_{2a}$). $AlPcS_{2a}$ contains a large number of isomers potentially with batch-to-batch variations that might lead to differences in biological effects upon exposure to light [50]. A new chemical entity was needed for clinical use, and on this basis $TPCS_{2a}$ was developed. The synthesized $TPCS_{2a}$ contains 3 isomers with low inter-batch variations and appears to be the first photosensitizer with strong absorption of light in the "therapeutic window" (600-800 nm) for photodynamic therapy, optimal properties for PCI and suitability for clinical use [50].

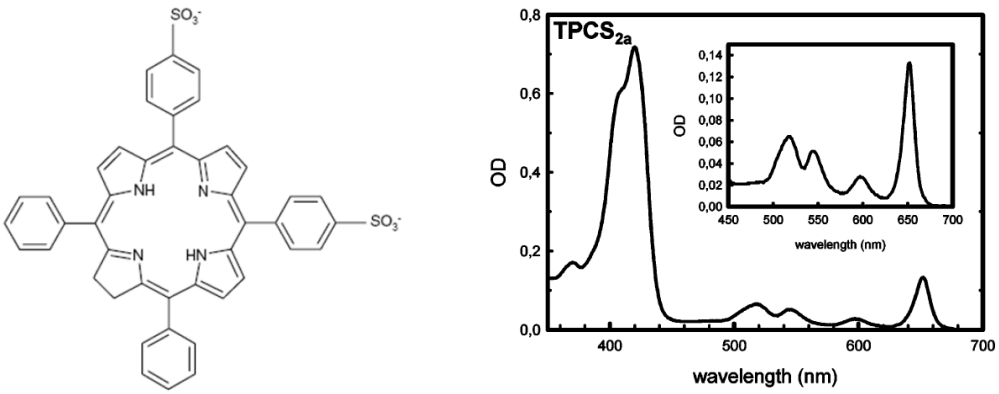

Figure 1.5: The figure shows the chemical structure and absorption spectra of $TPCS_{2a}$. Adapted from Berg *et al.* 2011 [50].

2 Materials and methods

2.1 Cell culture

2.1.1 Cell lines

In this study, three cell lines with different TP53 and MDM2 status were used: MES-SA (ATCC® CRL-1976™), SK-LMS1 (ATCC® HTB-88™) and SJSA-1 (ATCC® CRL-2098™). MES-SA is $TP53^{Wt}$ and MDM2 status is unknown. SK-LMS1 is $TP53^{Mut}$ and $MDM2^{Wt}$. SJSA-1 is $TP53^{Wt}$ and $MDM2^{Ampl}$.

Osteosarcoma cell line SJSA-1 was kindly provided by Professor Ola Myklebost (Department of Tumor Biology, The Norwegian Radium Hospital, Oslo). Uterine sarcoma cell line MES-SA and leiomyosarcoma cell line SK-LMS1 were both purchased from LGC Standards AB (Teddington, Middelsex, UK).

2.1.2 Culture medium

MES-SA was cultured in McCoy's 5a medium (Sigma-Aldrich, St. Louis, MO, USA) supplemented with L-glutamine, 10% fetal bovine serum (FBS) (PAA Laboratories, Pasching, Austria), 100 IU/ml penicillin (Sigma-Aldrich) and 100 µg/ml streptomycin (Sigma-Aldrich). SK-LMS1 was cultured in Dulbecco's modified Eagle's medium (DMEM) (Lonza Group Ltd, Basel, Switzerland) supplemented with L-glutamine, 10% FBS, 100 IU/ml penicillin and 100 µg/ml streptomycin. SJSA-1 was cultured in RPMI-1640 medium (Sigma-Aldrich) supplemented with L-glutamine, 100 IU/ml penicillin and 100 µg/ml streptomycin. All cell lines were cultured as monolayers in Nunclon™ surface treated tissue culture flasks (NUNC A/S, Thermo Fisher Scientific, Roskilde, Denmark) in incubators at 37°C and 5% v/v CO_2.

2.1.3 Splitting of cells

For optimal cell growth, it is important to make sure that the cells have enough nutrients and that the cells do not grow to confluence. This is done by checking the flasks in the microscope regularly. When the cells are approximately 80 % confluent (80 % of the flask's surface are covered by a cell monolayer), the cells should be split into new flasks. Up until this point the cells are in the log-phase of growth, while in a more confluent flask, the cells may stop growing or die.

Procedure

- Aspirate off the medium and rinse the cell layer with 2 ml Dulbecco's Phosphate Buffered Saline without Ca & Mg (PBS) (PAA Laboratories). The washing removes any remnants of trypsin-deactivating enzymes from the serum.
- Aspirate off the PBS, add 1 ml of 0,025%-0,5% trypsin/0,53 mM EDTA solution (Sigma-Aldrich), and incubate at 37ºC for a few minutes. Trypsin is a protease and will cleave the proteins attaching the cells to the surface of the flask.
- After incubation, give the flask a few gentle taps, and then study the flasks in the microscope to ensure that the cells are detached.
- Add 9 ml of pre-heated medium, and rinse the flask well by using the pipette
- Transfer the desired amount of cell suspension to a new flask and add pre-heated medium, e.g. ≈20 ml in 75 cm^2 flask and ≈40 ml in 175 cm^2 flask.

2.1.4 Counting of cells

To determine cell concentration prior to an experiment, cells were counted manually using a KOVA® Glastic Slide disposable plastic hemocytometer (Hycor Biomedical, Indianapolis, IN, USA).

Procedure

- Trypsinate the cell monolayer in one or more flasks and add pre-heated medium.
- Transfer 13 µl cell suspension to the hemocytometer chamber (if the cell suspension is dense, dilute the suspension to ease the counting)
- Count 3 squares in diagonal. Divide the number by three and then multiply by 10 000 to find the number of cells per ml

2.1.5 Optimisation of cell plating

Before starting the experiments, it was important to determine how many cells should be seeded per well of each cell line. This is done to avoid that the cells grow to confluence, which in turn can impair the growth of the cells and the reproducibility of the experiment. The procedure was designed to mimic a PCI experiment to give a realistic picture of how many cells we have in the control wells after five days.

Procedure

- In 96-well plates, 2000 – 20 000 cells per well with intervals of 2000 cells were seeded on day 1.
- On day 2, fresh medium was added. Following 18 hours incubation, the cells were washed twice with PBS and fresh medium was added.
- On day 5, viability was measured using the 3-[4,5-dimethylthiazol-2-yl]-2,5-diphenyl tetrazolium bromide (MTT) assay.

2.1.6 Growth curves

Growth curves were established for each of the 3 cell lines to determine the doubling time. This is useful in the planning of experiments to estimate how many cells should be seeded to obtain a certain number of cells.

Procedure

- On day 1, 150 000 cells were seeded in BD Falcon™ 3001 culture dishes (BD Biosciences, Franklin Lake, NJ, USA).
- After 24, 48, 72 and 96 hours, medium was aspirated, the dish washed once with PBS and 300 µl of trypsin was added.
- After a few minutes of incubation at 37°C and 5% v/v CO_2, 700 µl of medium was added and respectively 1, 0,5, 0,250, and 0,125 ml of the cell suspension was transferred to a small container and added coulter counter buffer to a total of 10 ml (Beckman Coulter Inc., Brea, CA, USA).
- The cell suspension was mixed before the cell number was determined using a Z2™ Coulter Counter® Cell and Particle Counter (Beckman Coulter Inc.).

2.1.7 Bleomycin

The cell lines' sensitivity to bleomycin was determined using the clonogenic assay (see 2.3.2)

Procedure

- On day 1, 400 cells per well of MES-SA, 600 cells per well of SJSA-1 and 800 cells per well of SK-LMS1 were seeded in 6-well plates and incubated overnight at 37°C and 5% v/v CO_2 to allow the cells to adhere.

- On day 2, medium containing none, 0,05, 0,1, 0,5, 1 and 5 IU/ml Bleomycin were added to the wells.
- Following 4-hour incubation, Bleomycin was removed and fresh medium was added.
- The cells were incubated for 7-10 days until colonies of >50 cells formed. The colonies where then dyed and counted manually.

2.1.8 Nutlin-3

For the SJSA-1 cell line, the growth inhibition curves of Nutlin-3 determined by Ohnstad *et al.* [1] were used. For MES-SA and SK-LMS1, the growth inhibition by Nutlin-3 was determined using the clonogenic assay (see 2.3.2).

Procedure

- On day 1, 400 cells of MES-SA and 600 cells of SJSA-1 were seeded in 6-well plates and incubated at 37°C and 5% v/v CO_2 overnight to allow the cells to adhere.
- On day 2, medium containing none, 0,1, 0,5, 1, 2,5 and 5 µM Nutlin-3 was added.
- On day 6, the cells were washed twice with PBS, and fresh medium was added.
- The cells were incubated for 7-10 days. The colonies where then stained and colonies consisting of >50 cells were counted manually (see 3.2.3).

2.2 PDT and PCI procedures

2.2.1 Light source and photosensitizer

PDT and PCI experiments were carried out using the LumiSource® light source (PCI Biotech AS, Oslo, Norway). The lamp is designed to provide homogenous irradiance over a defined illumination area of 45 x 17 cm. The lamp consists of four 18W Osram L 18/67 standard light tubes [53] emitting blue light with a peak wavelength of approximately 435 nm (figure 2.1).

The photosensitizer used in this study is $TPCS_{2a}$ (Amfinex®, PCI Biotech AS). $TPCS_{2a}$ is a disulfonated tetraphenyl chlorine developed by di-imide reduction of disulfonated tetraphenyl porphine ($TPPS_{2a}$). The synthesized $TPCS_{2a}$ contains 3 isomers and absorbs light at 652 nm [50]. The amphiphilic nature of the molecule allows it to be incorporated into the cell membrane, while a hydrophilic area ensures that the sensitizer does not penetrate through the membrane. $TPCS_{2a}$ localizes in endocytic vesicles, which is crucial for its use in photochemical internalization.

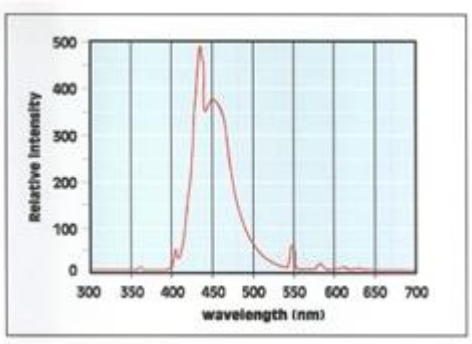

Figure 2.1: Emission spectrum from LumiSource® (PCI Biotech AS) [53]

2.2.2 PDT and PCI

PDT and PCI experiments were carried out in Nunc 96 MicroWell™ or 6-well plates (NUNC A/S, Thermo Fisher Scientific) or Nunclon™ cell culture flasks, 25cm^2 (NUNC A/S, Thermo Fisher Scientific) depending on the experiment. For western blotting, 6-well plates were used and for flow cytometry, 25 cm^2 flasks were used because of the need for a high number of cells for further analysis. Clonigenic assay used in all experiments with Bleomycin (Baxter International Inc, Deerfield, IL, USA) for assessing cytotoxicity was carried out in 6-well plates in order to ease the counting of colonies. The MTT assay was used to assess viability in experiments including Saporin (Sigma-Aldrich) and was carried out in 96-well plates.

PDT procedure

- For all experiments, the cells were seeded in the appropriate type of plates and left for ~24 hours to allow the cells to adhere.
- On day 2, the cells were incubated in medium containing 0,2 µg/ml $TPCS_{2a}$ for 18 hours
- On day 3, they were washed twice with PBS. Fresh medium was added, and the cells were chased for 4 hours to allow the photosensitizer to be internalized and cleared from the cell membrane.
- After the chase, the cells were illuminated using the LumiSource® lamp.

For PCI treatment, the protocol was identical to that for the PDT procedure with a few additional steps. For all experiments with Bleomycin, the drug was added after the removal of the photosensitizer, and was washed away after the 4-hour chase before illumination. In experiments with Saporin, the toxin was added with the photosensitizer and incubated for 18 hours before both substances were washed away.

2.3 Viability assays

2.3.1 MTT-assay

The MTT (3-[4,5-dimethylthiazol-2-yl]-2,5-diphenyl tetrazolium bromide) assay can be used to measure the viability of cells after a treatment. Since for most cell populations the total mitochondrial activity is related to the number of viable cells, this assay is broadly used to measure in vitro cytotoxic effects of drugs [54]. In viable cells, the yellow-colored tetrazolium salt MTT is converted into blue-colored formazan crystals by the mitochondrial enzyme succinate-dehydrogenase, which can be solubilised in different solutions such as methanol, ethanol, and DMSO [55]. Therefore, any increase or decrease in mitochondrial activity can be detected by measuring formazan concentration reflected in optical density (OD). The MTT-assay is an easy, sensitive and quick way of measuring acute cytotoxic effects of compounds [54].

Procedure

- Prepare a 0,25 mg/ml MTT solution by diluting a 5 mg/ml stock solution in suitable medium
- Aspirate off the medium from the wells. Add 100 µl MTT solution per well in 96-well plates, 1 ml in 6-well plates and 1 ml in BD Falcon™ 3001-dishes.
- On each plate, add MTT solution to one row of empty wells. This will serve as the blank control
- Incubate the plates at 37°C for ≈3-5 hours until visible formazan crystals are formed
- Aspirate off the MTT solution. Add 100 µl DMSO (Sigma-Aldrich) per well in 96-well plates, 1 ml per well in 6-well plates and in BD Falcon™ 3001-dishes.
- Gently shake for ≈5-10 minutes until the formazan crystals have dissolved
- For the 6-well plates and the 3001 dishes; transfer 100 µl to wells in a 96-well plate
- Measure the optical density at 570 nm using a Powerwave XS2 microplate spectrophotometer (BioTek, Winooski, VT, USA) and analyse the data using the Gen5™ Data Analysis Software (BioTek).

2.3.2 Clonogenic cell survival assay

A disadvantage of the MTT-assay is that the method can sometimes overestimate or underestimate cytotoxicity of a compound by not taking into account reversible damage or re-

growth of cells resistant to the drug/cytotoxic agent. It can also underestimate cellular damage and cell death because it works best for detecting the later stages of apoptosis [56]. For certain compounds, it might therefore be advisable to include clonogenic cell survival assays when determining in vitro cytotoxicity.

The clonogenic cell survival assay is a much-used method to measure the long-term cytostatic effects of a drug/cytotoxic agent. It allows us to determine the ability of a single cell to form a clone, proliferate and produce a viable colony [56]. In this study, clonogenic assay was used to measure cell survival in all experiments involving bleomycin, and a modified version of the protocol by Franken *et al*. [57] was utilised.

Procedure

- 400 cells per well of MES-SA, 600 cells per well of SJSA-1 and 800 cells per well for SK-LMS1 were seeded in 6-well plates, and treated according to the PDT and PCI protocols
- After 8-10 days depending on the cell line, visible colonies of at least 50 cells [57] were formed
- The medium was aspirated off and the colonies were washed once with 0,9% saline (Fresenius Kabi, Halden, Norway).
- The cells were fixed with ≈1 ml absolute ethanol (Kemetyl Norge AS, Vestby, Norway) for 10-30 minutes
- The ethanol was aspirated off. The colonies were stained with methylene blue for at least 5 minutes
- The methylene blue was aspirated off and the plates gently rinsed in tap water
- The plates were studied under the microscope to determine which colonies consisted of >50 cells. These colonies were counted manually

2.4 Analysis of protein expression by SDS-PAGE/Western blotting

In this study, analysis of protein expression by SDS-PAGE and western blotting were done to investigate the impact different treatments had on the expression of MDM2, p53, p21 and Bax.

2.4.1 Sample preparation

The experiments were carried out in 6-well plates to ensure enough proteins for the protein analysis. To avoid changes in growth that might affect the protein expression, it is important that the wells do not grow to confluence. 200 000 cells of SJSA-1 and 350 000 cells of MES-SA were seeded in each well. These numbers were determined based on the preliminary experiments on plating density.

Procedure

- At the desired time post treatment, put the dishes or 6-well plates on ice to stop any further cellular processes
- Aspirate off the medium. Ad 1 ml ice cold PBS without Mg^{2+} and Ca^{2+} and tilt the dish gently
- Aspirate off the PBS. Add 70 µl of lysis buffer (appendix A). Tilt the dish to cover the bottom
- Use a cell scraper to collect the lysate. Transfer the lysate to Eppendorf tubes
- Sonicate the tubes (4710 Series Ultrasonic Homogenizer, Cole-Parmer Instrument Co., Chicago, IL, USA). Vortex and spin down
- Allocate the lysate to Eppendorf tubes. Freeze at -80°C

2.4.2 Measurement of relative protein content

The relative protein content in the samples is measured to make the protein loading on the gel as even as possible.

Procedure

- Dilute 20 µl sample buffer (appendix A) 1:50 in dH_2O and 20 µl cell lysate 1:25 in dH_2O
- Wash a cuvette (black quartz, pathlength 10 mm, "Z" dimension 15 mm) twice with the diluted sample buffer. Then calibrate the spectrophotometer (Ultrospec 2100 pro UV/Visible, GE Healthcare Life Sciences, Uppsala, Sweden) with 80 µl of the buffer
- For each sample, wash the cuvette twice with 80 µl of the sample and then add 80 µl of the sample to the cuvette for measurements. Analyse each sample 3 times
- Calculate the mean protein content of the 3 parallels

- Fifteen µl of the sample with the lowest protein content will be applied on the gel. The other samples will be added in volumes to ensure that similar protein contents are added to each well.

2.4.3 Gel casting

The polyacrylamide gel is cast in two layers, the upper stacking gel and the main separating gel. The stacking gel has a low percentage (usually 3% w/v) of acrylamide through which proteins of all sizes readily migrate in the electric field. The purpose of the stacking gel is to "stack" all the proteins into a concentrated layer before entering the separating gel [58]. The separating gel has an acrylamide content of 5% - 17,5% depending on the size of the proteins to be studied. A higher acrylamide concentration gives smaller pores in the gel that in turn retards the proteins more. In this study, proteins ranging in size from 21 kDa to 60 kDa were studied. A gel with 12% acrylamide was chosen because this is optimal for the size range 14,4 – 65 kDa.

Procedure

- Wipe down the glass plates with 70% ethanol and set up the glass plate sandwich in the gel-casting stand. Make sure there are no leaks by wrapping the bottom half of the glass plate sandwich in Parafilm® M (Sigma-Aldrich)
- Mix all the components for the separating gel (appendix A) and the stacking gel (appendix A) except for APS and TEMED
- Add APS to the separating gel. Mix by inverting the tube a few times. Then add the TEMED and mix by inverting the tube a few times. The gel will now begin to polymerize
- Pipette the separating gel mix into the gel casting mould until the solution fills around ¾ of the mould
- Allow the gel to polymerize for 30-45 minutes
- Add APS to the stacking gel. Mix by inverting the tube a few times. Then add the TEMED and mix by inverting the tube a few times
- Pipette the stacking gel mix into the gel casting mould until it is full. Insert the comb into the top of the mould
- Allow the gel to polymerize for 20-30 minutes

- Use the gel immediately, or wrap it in Parafilm® M and aluminium foil and store it at 4ºC for up to a week.

2.4.4 SDS-PAGE

SDS-PAGE relies on the migration of charged molecules in a gel matrix in response to an electrical field. This technique facilitates the separation and resolution of a mixture of proteins according to molecular weight [58]. In this study, SDS-PAGE was carried out under reducing conditions. This involves the linearization of proteins by the dissociation of inter- and intrachain disulfide bonds, which is achieved by heating the protein sample briefly at 95ºC in the presence of the reducing agent dithiotreitol (DTT). The proteins are also coated with a negative charge in the presence of the anionic detergent SDS. They are then separated and resolved as discrete bands as they migrate in an electric field through the "sieving" action of the acrylamide gel matrix [58].

As a standard for protein size, a ladder consisting of a coloured component (Precision Plus Protein™ Kaleidoscope, Bio-Rad Laboratories, Hercules, CA, USA) and a protein component (Biotinylated Protein Ladder, Cell Signaling Technology, Danver, MA, USA) were applied on the gel alongside the samples. The coloured ladder allows us to see how the proteins migrate on the gel, and can be used as a visual control that the protein transfer from the gel to the membrane was successful. The protein ladder is visible on the developed western blot, and allows us to check the size of the proteins in our samples.

Procedure

- Prepare the ladder; 2 parts Kaleidoskop (Bio-Rad), 1 part Biotinylated ladder (Cell Signaling) and 2 parts sample buffer
- Pierce a hole in the tubes with sample and ladder. Heat at 95°C for 5 minutes
- Put the tubes on ice. Vortex and spin down
- Apply 10 µl ladder and the appropriate amount of sample on the gel
- Fill the chamber with running buffer (appendix A). Run the gel electrophoresis on ice at 200 V and 400 mA for ≈45 minutes

2.4.5 Western Blotting

After the proteins have been separated on the gel, they have to be transferred to a nitrocellulose or polyvinylidene difluoride (PVDF) membrane before they can be probed for

reactivity with different types of affinity reagents, such as antibodies [59]. This process is called western blotting, and usually takes place in a semidry buffer system using wetted filter papers sandwiched between planar electrodes. In this study, PVDF membranes (GE Healthcare Life Sciences) were used because of their high protein binding capacity, physical strength and chemical stability [60]. The membrane is extremely hydrophobic, and must therefore be pre-wetted in methanol prior to submersion in transfer buffer.

Procedure

- Soak a polyvinylidene difluoride (PVDF) membrane in methanol and then in the transfer buffer (appendix A)
- Assemble the blotting cassette as follows: pad, filter paper, gel, membrane, filter paper, pad (figure 2.2).
- Position the cassette in a blotting tank put on ice with a magnetic stirrer. Fill the tank with transfer buffer
- Run the blotting at 100 V and 400 mA for 2 hours at 4°C

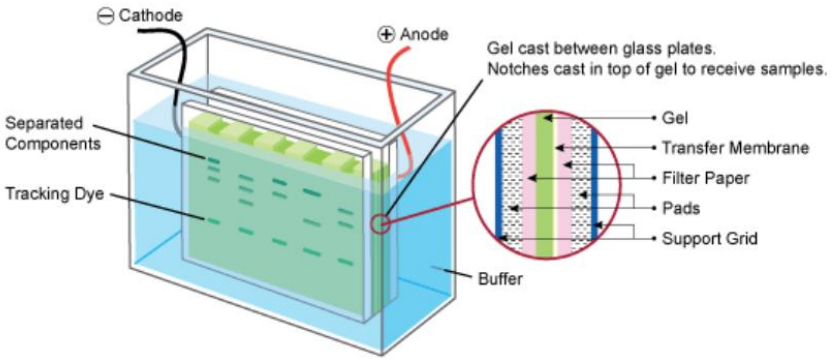

Figure 2.2: Illustration of the electrophoretic protein transfer from the polyacrylamide gel to the PVDF membrane. The proteins migrate to the membrane following a current that is generated by applying a voltage across the electrodes. Figure adapted from Leinco Technologies, Inc. [61]

2.4.6 Immunodetection

After transfer, the excess protein binding sites on the membrane must be blocked to avoid non-specific binding of antibodies. This can be done with solutions of proteins such as bovine serum albumin, non-fat dry milk or casein [59]. Following blocking, probing with antibodies is done in two steps; first with the primary antibody and then with the secondary antibody. The primary antibody binds to antigens on the membrane, and the secondary antibody binds

to the Fe-region on the primary antibody [59]. For this study, the recommendations for protein solutions from the antibody manufacturers were followed (appendix B).

Procedure

- Wash the membrane 3 x 10 minutes with 12 ml 1x TTBS (appendix A)
- Block the membrane with 15 ml 5% w/v non-fat dry milk (appendix A) for 1 hour at room temperature
- Incubate the membrane with primary antibody diluted in 5 ml 5% w/v non-fat dry milk or 5% w/v BSA (appendix A) overnight at 4°C
- Wash the membrane 3 x 10 minutes with 12 ml 1x TTBS
- Incubate the membrane with secondary antibody diluted in 5 ml 5% w/v non-fat dry milk for 1 hour at room temperature. Use anti-rabbit antibody for primary antibodies of rabbit origin etc. Use anti-biotin for the ladder

The secondary reagents are conjugated with an enzyme, usually horseradish peroxidase (HRP) or alkaline phosphatase (AP). HRP catalyses the oxidation of the luminol in the chemiluminescent substrate (LumiGLO®, KLP Inc., Gaithersburg, MD, USA), subsequently producing an excited state product that emits light [60]. The light is captured on an x-ray film (Amersham Hyperfilm ECL, GE Healthcare Life Sciences), and this film is then developed. The light emitted is proportionate with the amount of protein, so the blots can be quantified by comparing the bands in the different lanes.

Procedure

- Wash the membrane 3 x 10 minutes with 12 ml 1x TTBS
- Incubate with 1ml LumiGlo A and LumiGlo B (1:1) for 5 minutes at room temperature
- Fix the membrane between 2 transparent sheets in an exposure cassette. Gently smooth out any air pockets
- Place an x-ray film on top of the membrane, close the cassette and leave it for the desired exposure time
- Develop the film using the Agfa Curix 60 Film Processor (Agfa-Gevaert N.V., Mortsel, Belgium)

2.5 Flow cytometry

2.5.1 Principle

Flow cytometry is a technology in which a variety of measurements are made on cells, cell organelles, and other objects suspended in a liquid. Cells in suspension are made to flow one at a time through a sensing region of a flow chamber (flow cell) where measurements are made [62]. In the flow chamber, the cells are exposed to monochromatic light, usually from a laser, that upon hitting the cells scatter in all directions. Analysis of the scattered light provides information about the cell size and structure. The intensity of the forward-scattered light correlates with cell size. The intensity of the side-scattered light correlates with granularity, refractiveness and the presence of intracellular structures that can reflect the light [63]. Scattered light is collected via optics that directs the light to a series of filters and mirrors that isolate particular wavelength bands. The light signals are detected and digitalized for further analysis [64].

Flow cytometry measures optical and fluorescence characteristics of single cells. Physical properties, such as size and internal complexity can be used to distinguish certain cell populations. Fluorescently labelled antibodies can be used to identify a large number of cell surface and cytoplasmic antigens. Fluorescent dyes that incorporate into the DNA helical structure are used for measurement of cellular DNA content. The fluorescent signal is directly proportional to the amount of DNA in the nucleus, and can identify gross gains or losses in DNA [64].

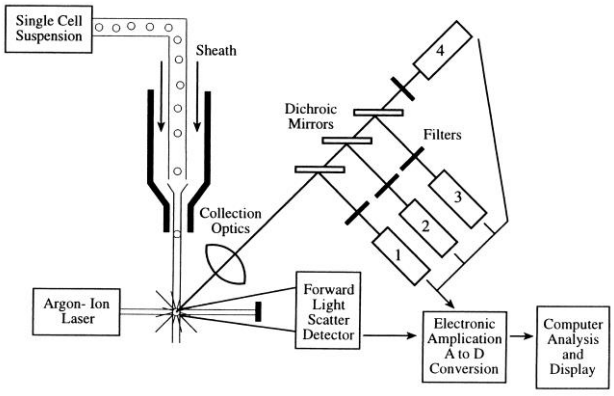

Figure 2.3: Example of the schematic of a flow cytometer. A single cell suspension is hydrodynamically focused with sheath fluid to intersect an Argon-Ion laser. Signals are collected by a forward angle light scatter detector, a side scatter detector (1), and multiple fluorescence emission detectors (2-4). The signals are amplified and converted to digital form for analysis and display on a computer screen [10].

2.5.2 Sample preparation

The experiments were carried out in 25 cm^2 flasks to ensure enough cells for further analysis. To avoid changes in growth that might affect the results, it is important that the flasks do not grow to confluence. In the flasks that were to receive PDT or PCI treatment, 500 000 cells were seeded. In the remaining flasks, 300 000 cells were seeded. The difference in plating density is due to the amount of cells that are lost during PDT and PCI treatment. The cells were treated according to the PDT and PCI protocol and harvested 2 and 20 hours post treatment.

Procedure

- Aspirate off the medium and wash once with 500 µl PBS. Transfer both medium and PBS to flow tubes
- Add 500 µl trypsin and leave in the incubator for a few minutes. Check in the microscope that the cells are detached
- Add 500 µl PBS and transfer to the flow tubes with the medium and the PBS
- Centrifuge at 2000 rpm for 4 minutes
- Aspirate off the supernatant and add 4 ml of PBS
- Centrifuge at 2000 rpm for 4 minutes
- Aspirate off the PBS and re-suspend in 500 µl ice cold methanol.

2.5.3 Analysis

In this study, flow cytometry was used for cell cycle analysis, study of DNA double strand breaks and to estimate the number of apoptotic cells after PDT and PCI treatment with or without added Nutlin-3. The fixed cells were first incubated with the TdT reaction solution. The components of this solution make up the TUNEL-assay, which is an assay that can identify cells undergoing apoptosis by labelling the ends of degrading DNA with the polymerase terminal deoxynucleotidyl transferase (TdT). When labelled nucleotides are incorporated by TdT, nuclei with degrading DNA can easily be detected by standard immunohistochemical or immunofluorescent techniques [65]. To detect DNA double strand breaks, the cells were incubated with γH2AX antibody (Millipore Corporation, Billerica, MA, USA). When DNA is damaged and DNA double strand breaks occur, the histone H2AX is phosphorylated and γ-H2AX foci are formed. These foci represent DNA double strand breaks in a 1:1 manner, and can therefore be used as a biomarker for such damage [66].

Finally, the cells are stained with Hoechst 33258. Hoechst is a fluorescent dye that stains DNA. The basis for the cell cycle analysis is measurement of DNA content in the cell, because this varies throughout the cell cycle. To ensure uniformity of single cell suspensions and remove cell aggregates, the suspension is filtered into BD Falcon™ tubes (BD Biosciences) through a 35 µm nylon mesh (BD Biosciences). The samples were analysed by the staff at the flow cytometry core facility on a BD LSR II Flow Cytometer (BD Biosciences).

Procedure

- Wash once with ≈4 ml PBS (centrifuge at 2000 rpm for 4 minutes)
- Add 35 µl TdT reaction solution (appendix A), incubate at 37°C for 30 minutes
- Wash once with PBS
- Add 50 µl 5% dry milk in PBS with 1/500 mouse α-γH2AX and 1/500 rabbit α-P-Histone H3. Incubate at room temperature for 30 minutes
- Wash twice with PBS
- Add 50 µl 5% dry milk in PBS with 1/50 goat α-rabbit-PE, 1/50 rabbit α-mouse-FITC and 1/400 streptavidine-Cy5. Incubate at room temperature for 30 minutes
- Wash once with PBS and add 300 µl 1,5 µg/ml Hoechst 33258. Incubate at room temperature for 30 minutes
- Filter and transfer to appropriate tube before analysis

3 Results

3.1 Growth curves and density curves

For optimal results of many experiments, including viability assays, it is important that the cells do not grow to confluence. When the cells approach confluence, the growth rate decreases, and cells may start to die. Growth curves and density curves were therefore obtained for the three cell lines SK-LMS1, MES-SA and SJSA-1 to determine optimal plating density.

3.1.1 Density curves

The cells were seeded out at different cell densities in 96-well plates, and the optical density was measured 5 days post plating using the MTT assay as described in 2.3.1.

The density curves for SK-LMS1 (figure 3.1A) and MES-SA (figure 3.1B) cells show linear growth up to approximately 12 000 cells seeded per well. When more than 12 000 cells were seeded in each well in a 96-well plate, the curve levelled off indicating non-exponential growth. For later experiments, SK-LMS1 and MES-SA cells were therefore seeded at a density of 4000 cells per well. The density curves for SJSA-1 (figure 3.1C) show linear growth up to approximately 10 000 cells seeded. To avoid confusion, 4000 cells per well in 96-well plates were also seeded of SJSA-1 cells. This number is low enough to avoid the cells growing confluent, while ensuring enough cells for detection by the MTT assay.

3.1.2 Growth curves

For experiments involving western blotting or flow cytometry, it is crucial to isolate a high number of cells. It is therefore important to seed enough cells in the beginning of the experiment, but not so many that the cells grow to confluence. Growth curves (figure 3.1D) were obtained to study the doubling time of the different cell lines, to determine how many cells to seed for the experiments. Estimated doubling time (Td) for SK-LMS1 was 30 hours, 27 hours for SJSA-1 and 20 hours for MES-SA.

Doubling time (Td) was calculated using the following formula [67]:

$$Td = \frac{t \times \ln 2}{\ln(N_t / N_0)}$$

Where t is the duration of the exponential growth phase, N_t is the number of cells after the exponential phase and N_0 is the number of cells before the exponential phase.

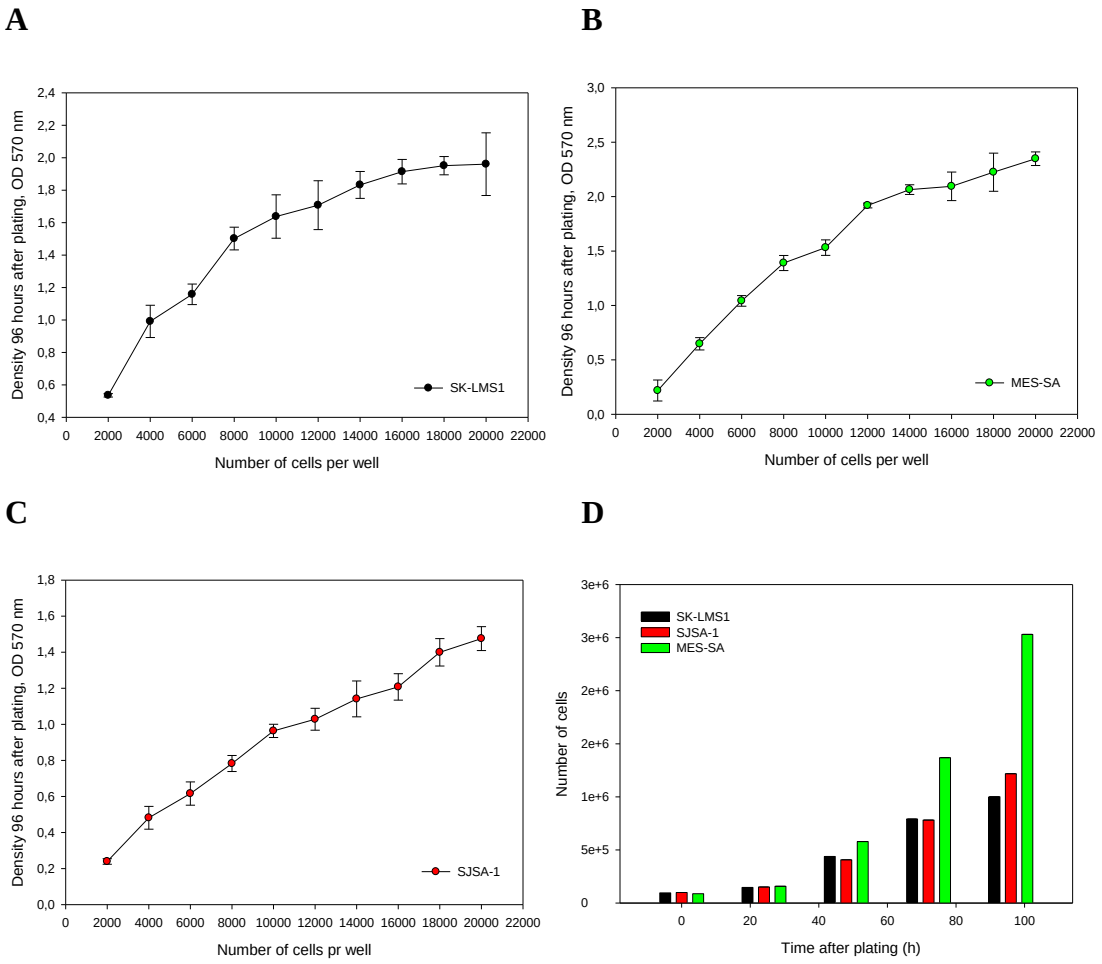

Figure 3.1: Density curves for SK-LMS1 **(A)**, MES-SA **(B)** and SJSA-1 **(C).** The optical density at different plating densities was measured with the MTT assay. **D:** Growth curves for SK-LMS1, MES-SA and SJSA-1. The number of cells was counted 0, 24, 48, 72 and 96 hours post plating. All figures show a representative result from a single experiment. Error bars represent the empiric standard deviation (n=3).

3.2 Bleomycin sensitivity

Before initiating experiments with bleomycin, the three cell lines were tested using the clonogenic assay to determine their bleomycin sensitivity. Bleomycin is a slow acting chemotherapeutic agent, and requires many days to fully exert its therapeutic potential. Thus, the therapeutic effect of bleomycin is usually assessed by a clonogenic assay. In 6-well plates, 400 cells per well of MES-SA, 600 cells per well of SJSA-1 and 800 cells per well of SK-LMS1 were seeded and treated with 0 – 5 IU/ml Bleomycin for 4 hours. The cells were then incubated for 8-10 days until visible colonies were formed, the colonies were stained

and counted manually. The surviving fraction was calculated and LD_{50} was estimated. For MES-SA (figure 3.2B), LD_{50} was approximately 0,1 IU/ml bleomycin and for SK-LMS1 (figure 3.2A) and SJSA-1 (figure 3.2C) LD_{50} was approximately 0,3 IU/ml.

A **B**

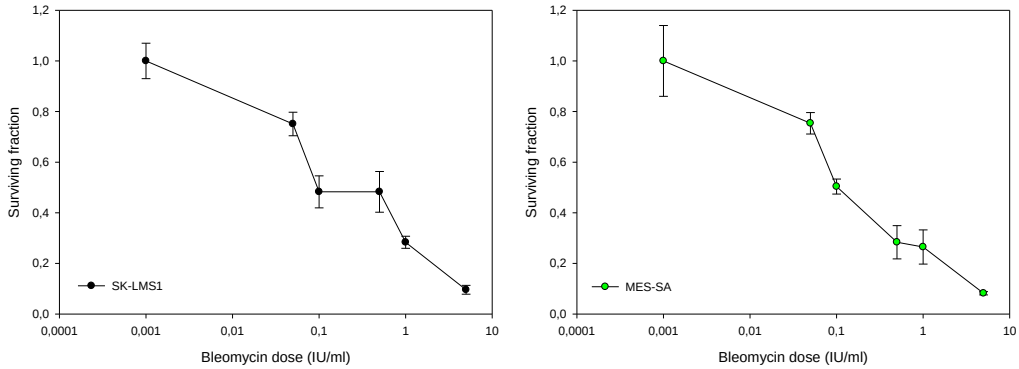

C

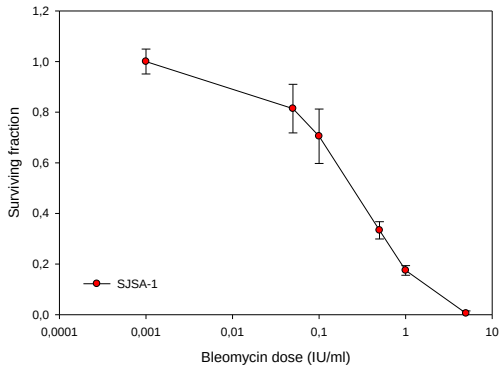

Figure 3.2: Bleomycin sensitivity of SK-LMS1 **(A)**, MES-SA **(B)** and SJSA-1 **(C)**. All figures show a representative result from a single experiment. Error bars represent the empiric standard deviation (n=3).

3.3 PDT and PCI with $TPCS_{2a}$

3.3.1 PDT and PCI with $TPCS_{2a}$ and saporin

The results of PDT and PCI treatment of SK-LMS1, MES-SA and SJSA-1 cells are shown in figure 3.3-3.5. To study the effect of treatment with saporin the MTT assay was utilised, and 4000 cells per well in 96-well plates were seeded. The cells receiving PDT were incubated with 0,2 µg/ml $TPCS_{2a}$. The cells receiving PCI treatment were incubated with 0,2 µg/ml $TPCS_{2a}$ and 0,06 µg/ml, 0,3 µg/ml or 1,0 µg/ml saporin. Following the 18-hour incubation with $TPCS_{2a}$ with or without saporin, the cells were chased for 4 hours, treated with light doses ranging from 0 - 250 seconds (0 - 2,675 J/cm^2) and examined by the MTT assay 48 hours post light. There were great differences in the response to the treatment in the 3 cell lines.

The PCI effect was calculated using the following formula:

$$\frac{\frac{1}{D_{20}\ PCI}}{\frac{1}{D_{20}\ PDT}}$$

MES-SA cells responded well to PDT (figure 3.4). To reduce the viability to 20%, a light dose of 110 seconds was necessary. SK-LMS1 (figure 3.3) and SJSA-1 (figure 3.5) cells were less sensitive to PDT, requiring a light dose of 240 and 175 seconds respectively to induce the same loss of viability. The cells response to PCI treatment was stronger. To induce an 80% loss of viability when treated with PCI of 0,06 µg/ml saporin, SK-LMS1 cells required a light dose of 95 seconds (figure 3.3A), MES-SA cells 20 seconds (figure 3.4A) and SJSA-1 cells 15 seconds of light exposure (figure 3.5A). The PCI effect was therefore 2,53 in SK-LMS1 cells, 5,5 in MES-SA cells and 11,67 in SJSA-1 cells.

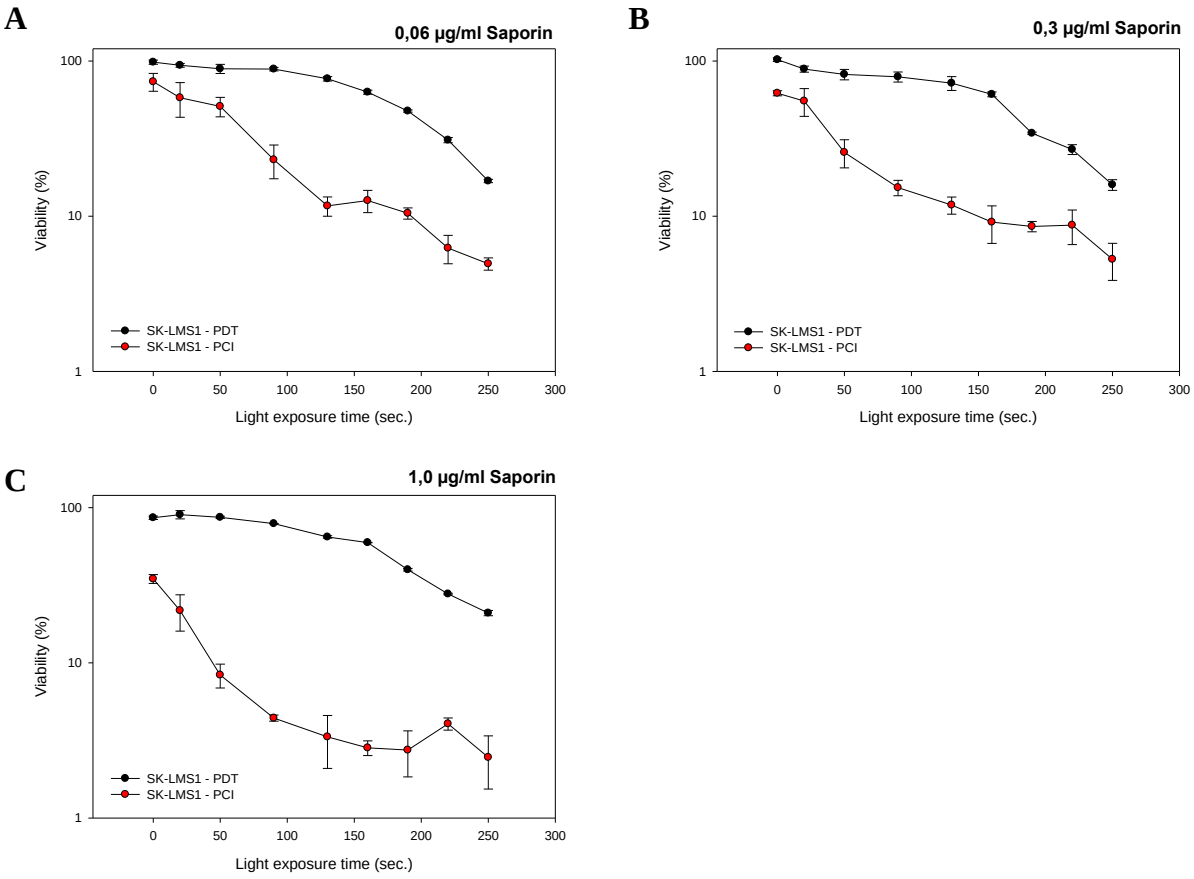

Figure 3.3: PDT and PCI of SK-LMS1 cells with 0,06 µg/ml **(A)**, 0,3 µg/ml **(B)** and 1,0 µg/ml **(C)** saporin and increasing light dose. All figures show a representative result from a single experiment. Error bars represent the empiric standard deviation (n=3).

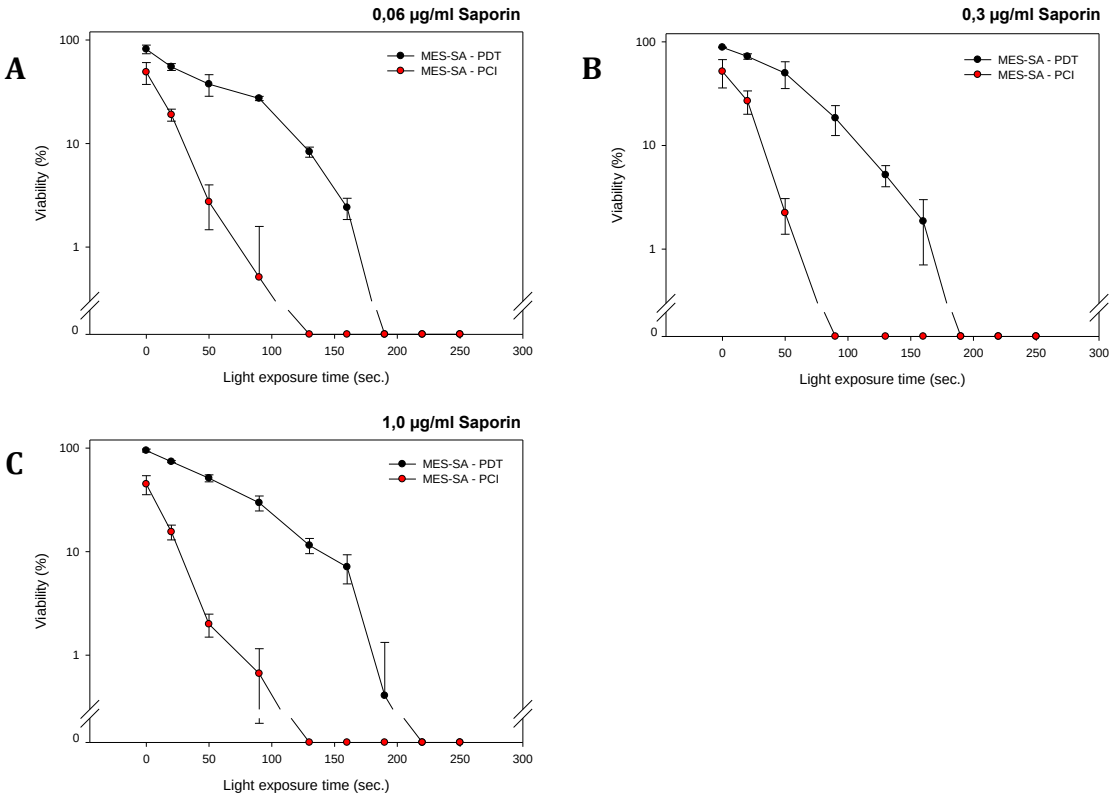

Figure 3.4: PDT and PCI of MES-SA cells with 0,06 µg/ml **(A)**, 0,3 µg/ml **(B)** and 1,0 µg/ml **(C)** saporin and increasing light dose. All figures show a representative result from a single experiment. Error bars represent the empiric standard deviation (n=3).

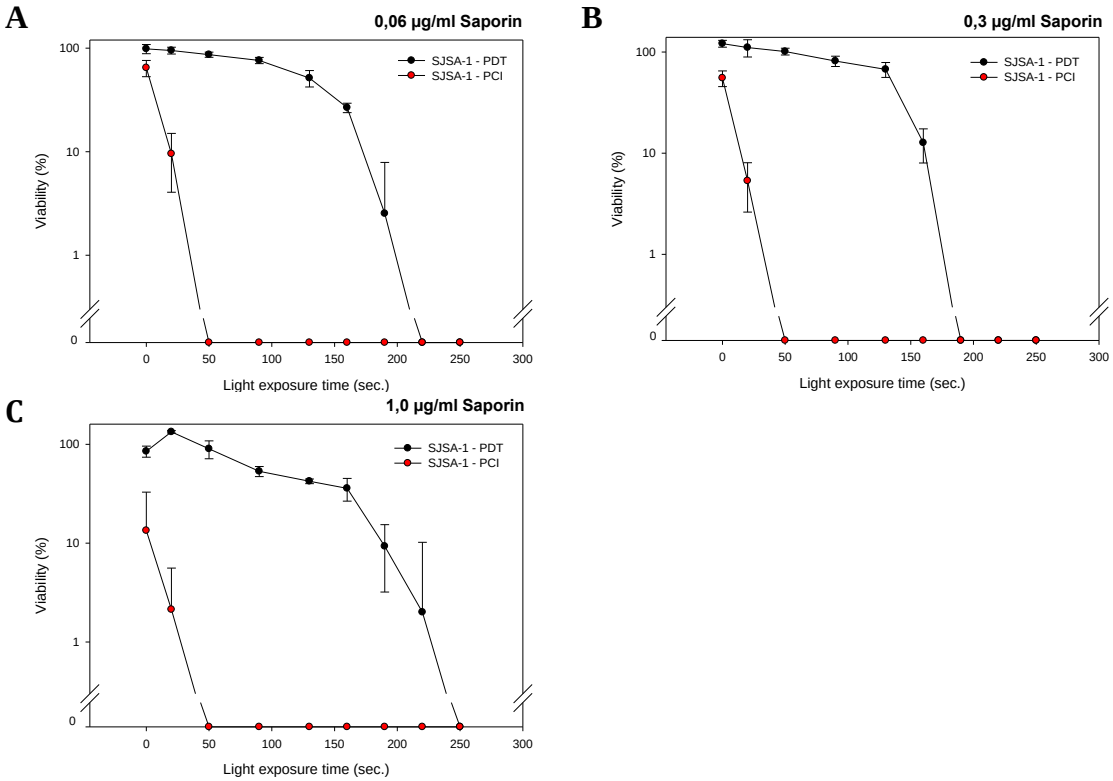

Figure 3.5: PDT and PCI of SJSA-1 cells with 0,06 µg/ml **(A)**, 0,3 µg/ml **(B)** and 1,0 µg/ml **(C)** saporin and increasing light dose. All figures show a representative result from a single experiment. Error bars represent the empiric standard deviation (n=3).

3.3.2 PDT and PCI with $TPCS_{2a}$ and bleomycin

The results of PDT and PCI treatment of SK-LMS1, MES-SA and SJSA-1 cells are shown in figure 3.6. To study the effect of treatment with bleomycin the clonigenic assay was utilised. 800 cells per well of SK-LMS1 and 600 cells per well of SJSA-1 were seeded in 6-well plates and 1000 cells of MES-SA per 25 cm^2 flask were seeded. The cells receiving PDT were incubated with 0,2 µg/ml $TPCS_{2a}$. The cells receiving PCI treatment were incubated with 0,2 µg/ml $TPCS_{2a}$ for 18 hours and different doses of Bleomycin for 4 hours. MES-SA and SJSA-1 cells was treated with 0,1 IU/ml Bleomycin and SK-LMS1 cells with 0,3 IU/ml Bleomycin. The cells received light doses ranging from 0 – 150 seconds (0 - 1,605 J/cm^2). After 10 days, the colonies were stained and counted manually.

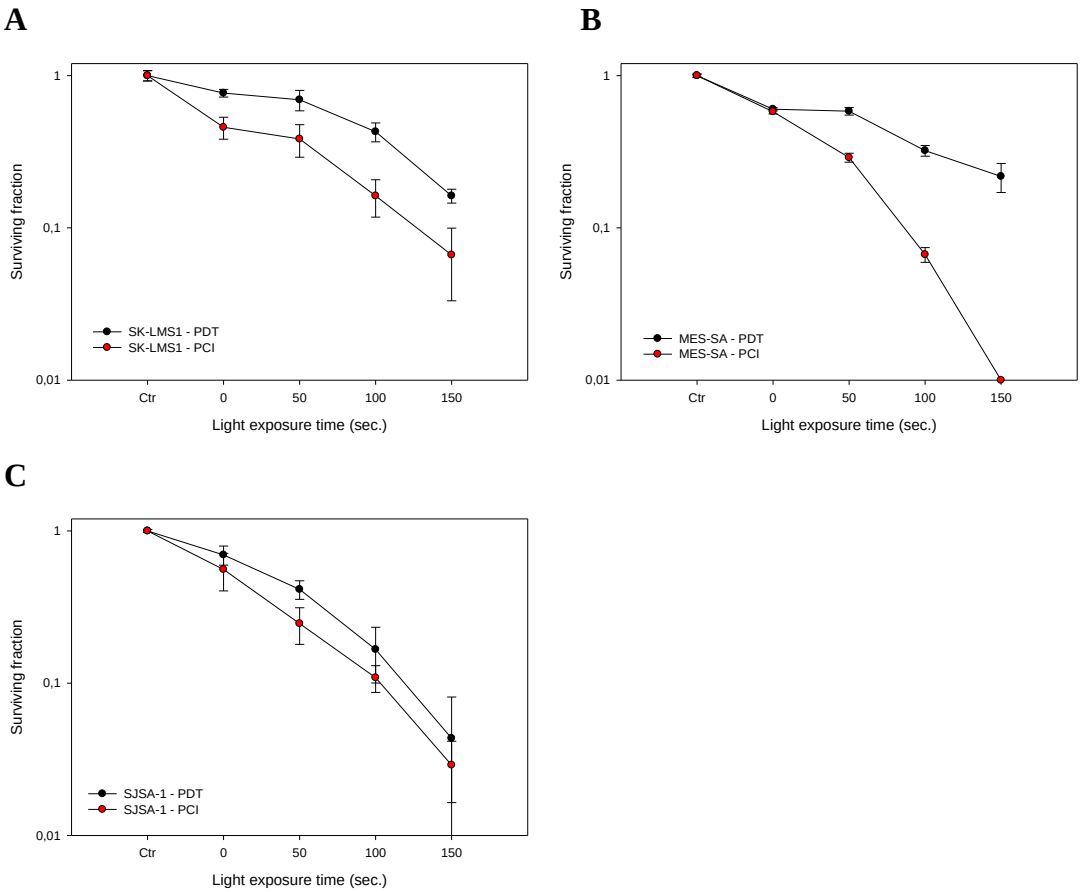

Figure 3.6: Clonogenic survival after PDT and PCI treatment of **A:** SK-LMS1 with 0,3 IU/ml bleomycin **B:** MES-SA with 0,1 IU/ml bleomycin **C:** SJSA-1 with 0,1 IU/ml bleomycin. All figures show a representative result from a single experiment. Error bars represent the empiric standard deviation (n=3).

SK-LMS1 (figure 3.6A) and MES-SA (figure 3.6B) cells had similar response to PDT requiring light doses of 145 and 150 seconds respectively to induce an 80% loss of viability. SJSA-1 cells (figure 3.6C) appear to be the most sensitive of the three cell lines to PDT with a light dose of 95 seconds required to reduce the viability to 20%. The viability of both MES-SA and SJSA-1 cells was reduced to 20% when treated with PCI of 0,1 IU/ml bleomycin and a light dose of 70 seconds. SK-LMS1 cells appear to be less sensitive to PCI treatment than the two other cell lines, requiring a light dose of 90 seconds to induce an 80% loss of viability when treated with PCI of 0,3 IU/ml bleomycin.

When comparing the PCI effects on the three cell lines, it is important to bear in mind that SK-LMS1 cells were treated with 0,3 IU/ml bleomycin, while SJSA-1 and MES-SA cells were treated with 0,1 IU/ml bleomycin. The PCI effect of SK-LMS1 cells can therefore not be compared with the PCI effect of the other two cell lines. The PCI effect was 1,61 in SK-LMS1 cells, 2,14 in MES-SA cells and 1,36 in SJSA-1 cells.

3.3.3 PDT and PCI with $TPCS_{2a}$ and saporin ± Nutlin-3

The effect Nutlin-3 had on the cell survival after PDT and PCI treatment with $TPCS_{2a}$ and saporin were studied using the MTT assay (figure 3.7). SJSA-1 cells were seeded out in 96-well plates with a plating density of 4000 cells per well. The cells were incubated with 0,2 μg/ml $TPCS_{2a}$ and 0,06 μg/ml, 0,03 μg/ml or 0,01 μg/ml saporin. Lower doses of saporin were used for this experiment because the previous experiment on SJSA-1 cells with saporin showed high toxicity of saporin in this cell line. Following an 18-hour incubation, the photosensitizer and saporin was washed away with PBS without Ca & Mg. Half the wells were added 500 nM Nutlin-3, which was not removed until immediately before MTT. After 4 hours, the cells were treated with light doses ranging from 0 - 250 seconds (0 - 2,675 J/cm^2) and examined by the MTT assay 48 hours post treatment.

This experiment showed very small differences in loss of viability between the PDT and PCI treated SJSA-1 cells that were incubated with 500 nM Nutlin-3, and those that were not. There seems to be bigger differences after PDT (figure 3.7A) than after PCI treatment (figure 3.7B-D), but the experiment needs to be repeated to confirm this. In the PCI treated cells there were no distinct differences in loss of viability between the saporin doses, but 0,01-0,06 μg/ml saporin induced a substantial loss of viability so it might be wise to repeat the experiments with lower doses of saporin, to better see any potential differences.

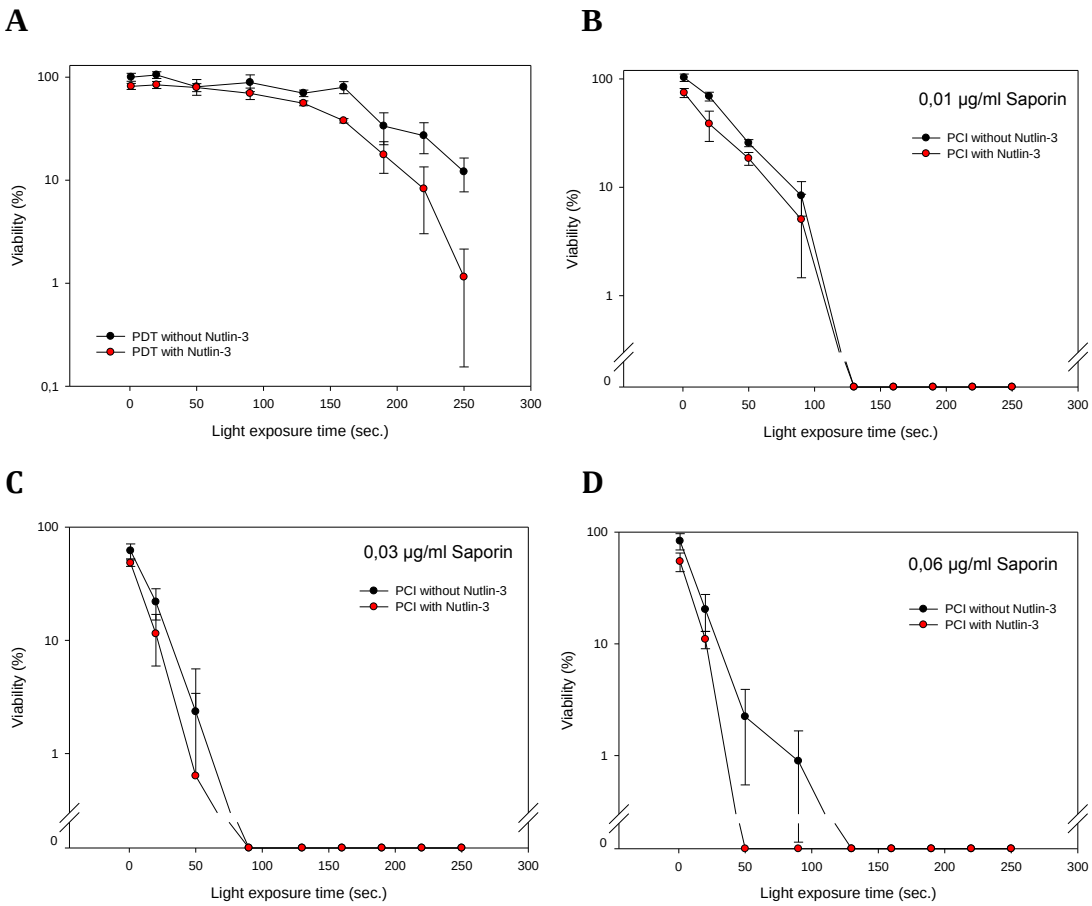

Figure 3.7: PDT **(A)** and PCI treatment of SJSA-1 cells with 0,01 µg/ml **(B)**, 0,03 µg/ml **(C)** and 0,06 µg/ml **(D)** saporin, with or without added 500 nM Nutlin-3. All figures show a representative result from a single experiment. Error bars represent the empiric standard deviation (n=3).

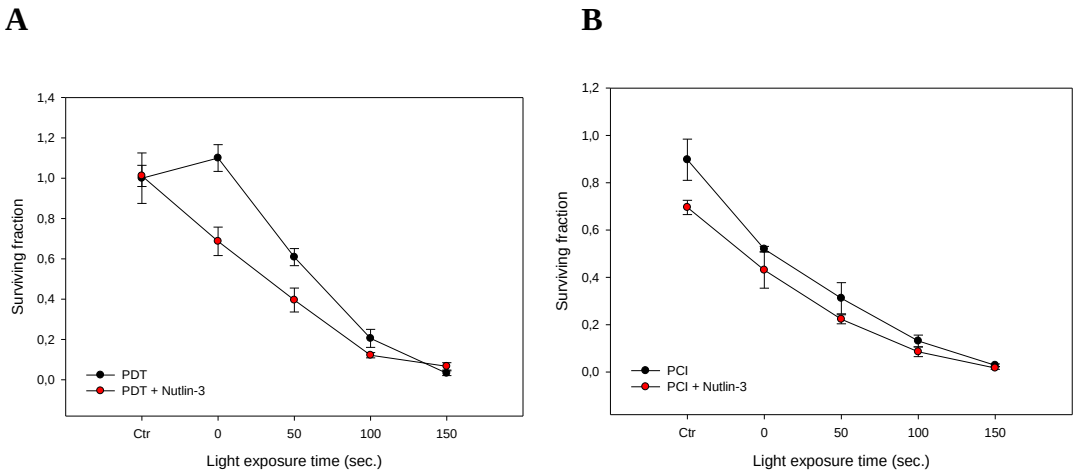

Figure 3.8: Clonogenic survival after PDT **(A)** and PCI **(B)** treatment with bleomycin of SJSA-1, with or without 500 nM Nutlin-3. All figures show a representative result from a single experiment. Error bars represent the empiric standard deviation (n=3).

3.3.4 PDT and PCI with $TPCS_{2a}$ and bleomycin ± Nutlin-3

The effect Nutlin-3 has on the cell survival after PDT and PCI treatment with $TPCS_{2a}$ and bleomycin was studied using the clonogenic assay (figure 3.8). SJSA-1 cells were seeded in 6-well plates with a plating density of 600-1200 cells per well. The cells to be treated with PDT and PCI were incubated with 0,2 μg/ml $TPCS_{2a}$ for 18 hours. The cells were then washed twice with PBS without Ca & Mg and 0,1 IU/ml Bleomycin were added to the wells to be treated with PCI or bleomycin only. Half of the wells were in addition treated with 500 nM Nutlin-3. After 4 hours, the Bleomycin was removed and half the wells were continued to be treated with 500 nM Nutlin-3 until the colonies were counted. The cells to be treated with PDT and PCI were treated with light doses ranging from 0 – 150 seconds (0 - 1,605 J/cm^2). After 10 days, the colonies were stained and counted manually.

Both for the PDT and PCI treated cells, there seem to be a greater loss in viability in the cells incubated with Nutlin-3. As in the experiment with Saporin, the difference appears to be greater in the PDT treated cells (figure 3.8A). This experiment has not been reproduced, so it needs to be repeated to confirm these results and to be able to quantify the differences.

3.4 Analysis of protein expression

To investigate the impact Nutlin-3 has on the p53 signalling, expression of p53, MDM2, p21 and Bax was measured by SDS-PAGE, western blotting and immunodetection (figure 3.9-3.12). In 6-well plates, 150 000 – 200 000 SJSA-1 cells per well were seeded and treated according to the PDT and PCI protocols. The cells to be treated with PDT and PCI were incubated with 0,2 μg/ml $TPCS_{2a}$ for 18 hours, before the photosensitizer was washed away with PBS without Ca & Mg. The PCI and BLM cohorts were then incubated with 0,1 IU/ml bleomycin for 4 hours before the PDT and PCI cohorts were illuminated for 160 seconds. During the chase period and until the cells were harvested, half the wells were treated with 500 nM Nutlin-3. The cells were harvested 8, 24 and 48 hours post light. The protein expression was measured according to the SDS-PAGE, western blotting and immunodetection protocols (section 2.4).

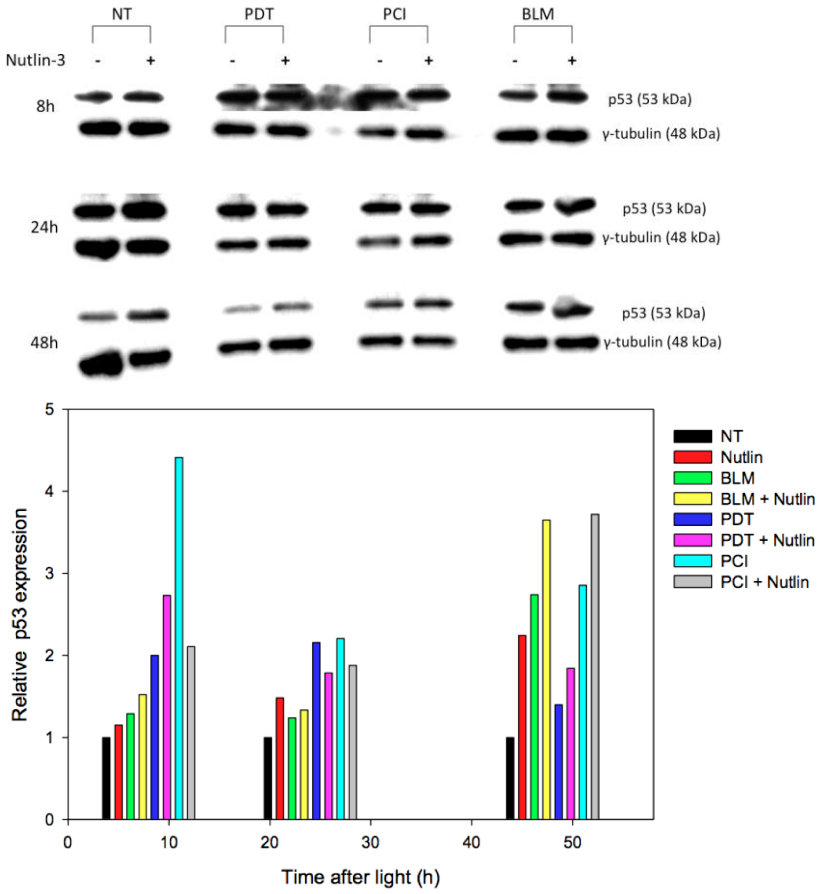

Figure 3.9: Expression of p53 in SJSA-1 cells after PDT, PCI and BLM treatment in the absence or presence of Nutlin-3. The results were normalised with respect to total γ-tubulin, relative to untreated cells. The figure shows the result from one experiment.

3.4.1 p53

The expression of p53 after PDT, PCI and bleomycin treatment was measured 8, 24 and 48 hours post light (figure 3.9). The level of p53 in the cells treated with only Nutlin-3 (red column) is higher than in the controls (black column), indicating that Nutlin-3 alone can increase p53 expression. The p53 expression in cells treated with bleomycin and Nutlin-3 (yellow column) is higher than for bleomycin treatment alone (green column), and the difference is most distinct after 48 hours. The p53 expression is higher in PCI treated cells (light blue column) than PDT treated cells (dark blue column) and the difference is most distinct 24 hours post light. The p53 expression was higher in the PDT and PCI treated cells that received Nutlin-3 treatment (pink and grey column respectively) than the cells receiving PDT and PCI treatment alone 48 hours post light. It appears that PCI treatment induces the highest expression of p53 8, 24 and 48 hours post light. PDT results in higher levels of p53

than bleomycin 8 and 24 hours post light, whereas after 48 hours bleomycin treatment gives a great increase in p53 expression higher than PDT.

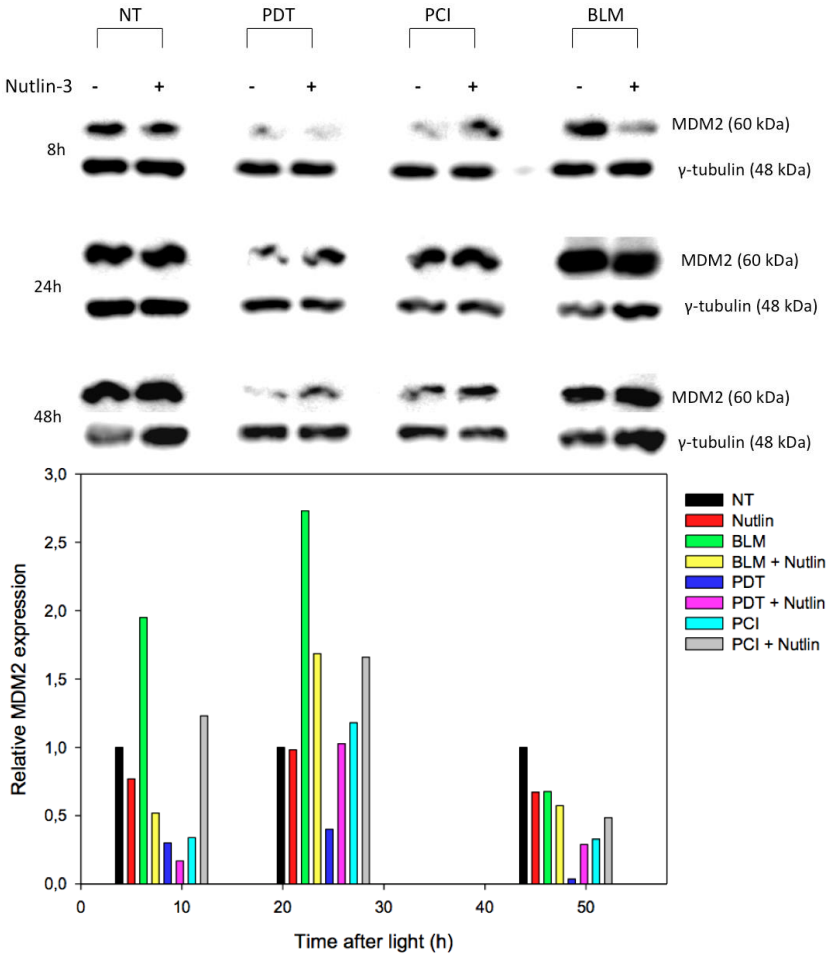

Figure 3.10: Expression of MDM2 in SJSA-1 cells after PDT, PCI and BLM treatment in the absence or presence of Nutlin-3. The results were normalised with respect to total γ-tubulin, relative to untreated cells. The figure shows the result from one experiment.

3.4.2 MDM2

The differences in expression of MDM2 (figure 3.10) show two tendencies. In bleomycin (green column) and untreated cells (black column) the level of MDM2 decreased when Nutlin-3 was added, while in PDT and PCI treated cells (dark blue and light blue column respectively) it increased after Nutlin-3 treatment. The expression of MDM2 is higher after 24 hours than 8 and 48 hours post light for all treatments. The MDM2 level was lower than in the control for many of the samples, and 48 hours post light all the samples expressed less MDM2 than the control.

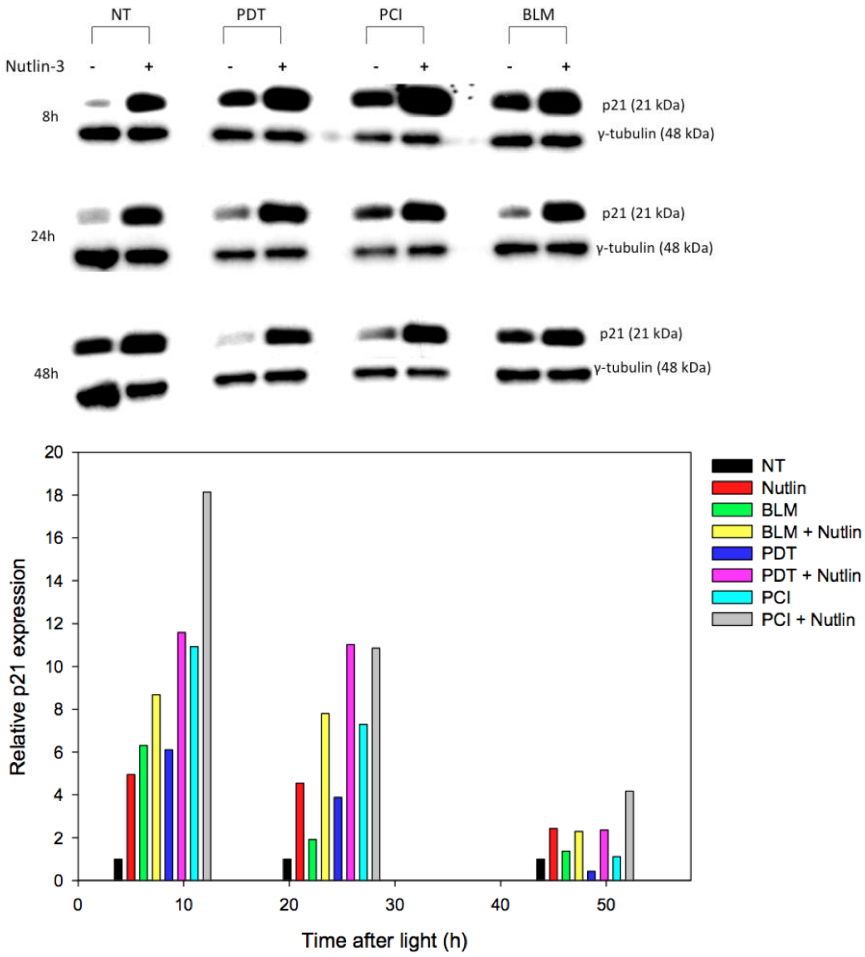

Figure 3.11: Expression of p21 in SJSA-1 cells after PDT, PCI and BLM treatment in the absence or presence of Nutlin-3. The results were normalised with respect to total γ-tubulin, relative to untreated cells. The figure shows the result from one experiment.

3.4.3 p21

To study the effect of Nutlin-3 treatment, the expression of downstream targets of p53 was measured by western blotting. An increase in p53 activity following an inhibition of the MDM2-p53 interaction may lead to increased expression of p21. For all treatments, the expression of p21 was considerably higher when Nutlin-3 was added (figure 3.11). The level of p21 increased 8 hours after light, and then decreased, indicating that the transcription of p21 is initiated ≤ 8 hours post light. The expression of p21 was higher in the PCI treated cells (light blue and grey column) than for the other treatments 8 to 48 hours post light. The expression of p21 is higher in the PDT treated cells (dark blue and pink columns) than the bleomycin treated cells (green and yellow columns) 24 hours post light, while 8 and 48 hours post light the expression in the bleomycin treated cells are slightly higher. The p21 levels in the cells treated with only Nutlin-3 (red columns) are higher than in the control (black

column) supporting the observation in 3.4.1 that Nutlin-3 alone can activate the p53 pathway, thereby inducing expression of the downstream target p21.

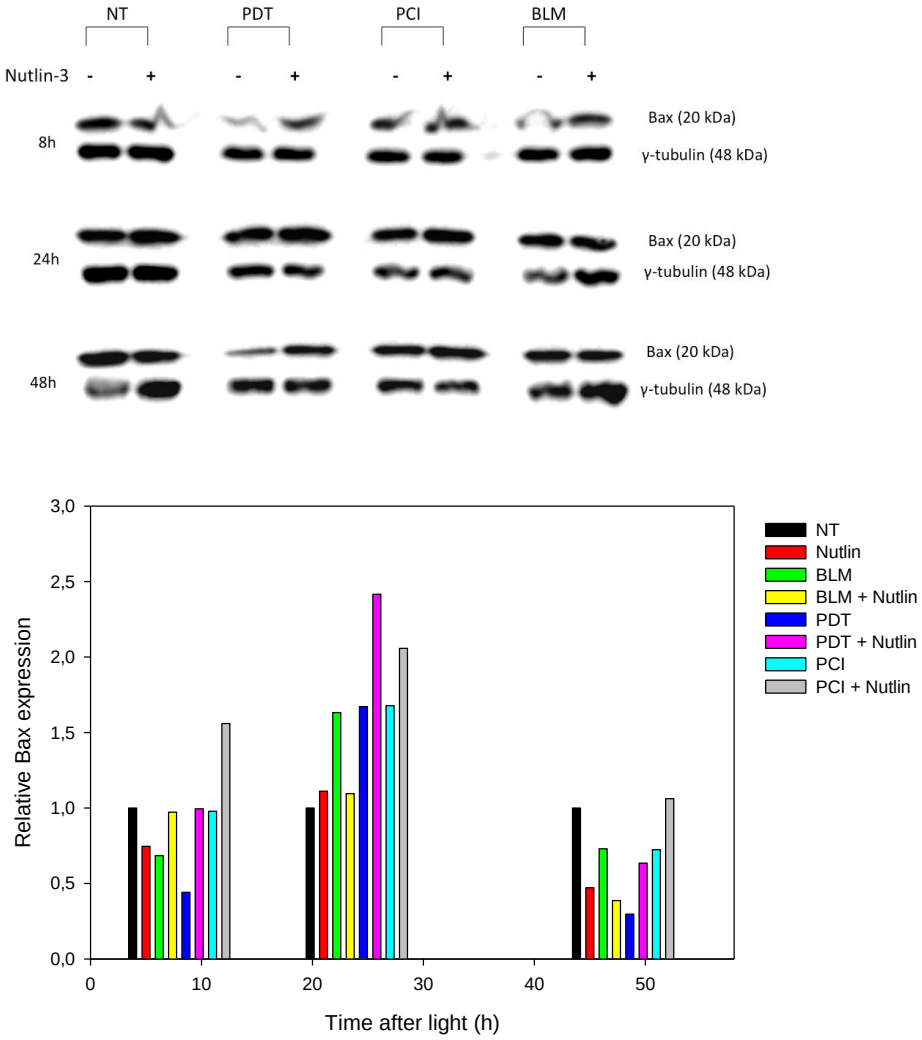

Figure 3.12: Expression of MDM2 in SJSA-1 cells after PDT, PCI and BLM treatment in the absence or presence of Nutlin-3. The results were normalised with respect to total γ-tubulin, relative to untreated cells. The figure shows the result from one experiment.

3.4.4 Bax

In this experiment, the medium in the dishes was removed before the monolayer was lysed. Any cells detached from the surface of the dish are therefore not included in this analysis. There is reason to believe that it might have had a significant impact on the expression of Bax since the treatments with the greatest loss in viability was observed with more cells detached from the surface of the dish, and may be apoptotic cells.

The expression of Bax appears to be higher in the PDT and PCI treated cells treated with Nutlin-3 than those not treated with Nutlin-3 (figure 3.12). The cells receiving

bleomycin treatment or no treatment did not show a clear correlation between Nutlin-3 treatment and Bax expression. The Bax level appears to be higher 24 hours post light than 8 and 48 hours post light.

3.5 Cell cycle analysis

The cell cycle distribution of SJSA-1 cells after PDT and PCI treatment with or without Nutlin-3 was analysed using flow cytometry. In 25 cm^2 flasks, 165 000 – 320 000 cells per flask were seeded and treated according to the PDT and PCI protocols. The PDT and PCI treated cells were incubated with 0,2 μg/ml $TPCS_{2a}$ for 18 hours before the PCI and BLM cohorts were incubated with 0,1 IU/ml bleomycin for 4 hours. Following the 4-hour chase, the PDT and PCI cohorts were illuminated for 160 seconds. From 4 hours before light until harvest half the cells were treated with 500 nM Nutlin-3. The cells were harvested 2 hours and 20 hours post light and prepared for analysis according to the flow cytometry protocol.

When genetic material is damaged, delay in cell cycle progression facilitates DNA repair and ensures genetic stability. The cell cycle checkpoints monitor the integrity and the replication status of the genome, and prevent cells with damaged DNA from entering the next phase in the cell cycle. The ability of the checkpoint to inhibit entry into S phase is closely related to the tumour suppressor p53 [18]. In cells with non-functional p53, due to mutations or MDM2 amplification, the cell cycle checkpoints will not function properly, and cells with damaged DNA might progress in the cell cycle.

The impact of adding Nutlin-3 on progression in the cell cycle in SJSA-1 cells was studied using flow cytometry. The cells harvested 2 hours post light showed very small differences in cell cycle (results not shown). In the samples harvested 20 hours post light (figure 3.13), greater differences were seen. In the PCI samples (figure 3.13D), a greater proportion of the cells treated with 500 nM Nutlin-3 were in G_1 and G_2 phase and fewer were in S phase than the cells only receiving PCI treatment. For the other treatments (figure 3.13A-C) the S-phase fraction appears to be approximately the same in the absence or presence of Nutlin-3, but there are more cells in G_1-phase after Nutlin-3 treatment than for the corresponding treatment without Nutlin-3.

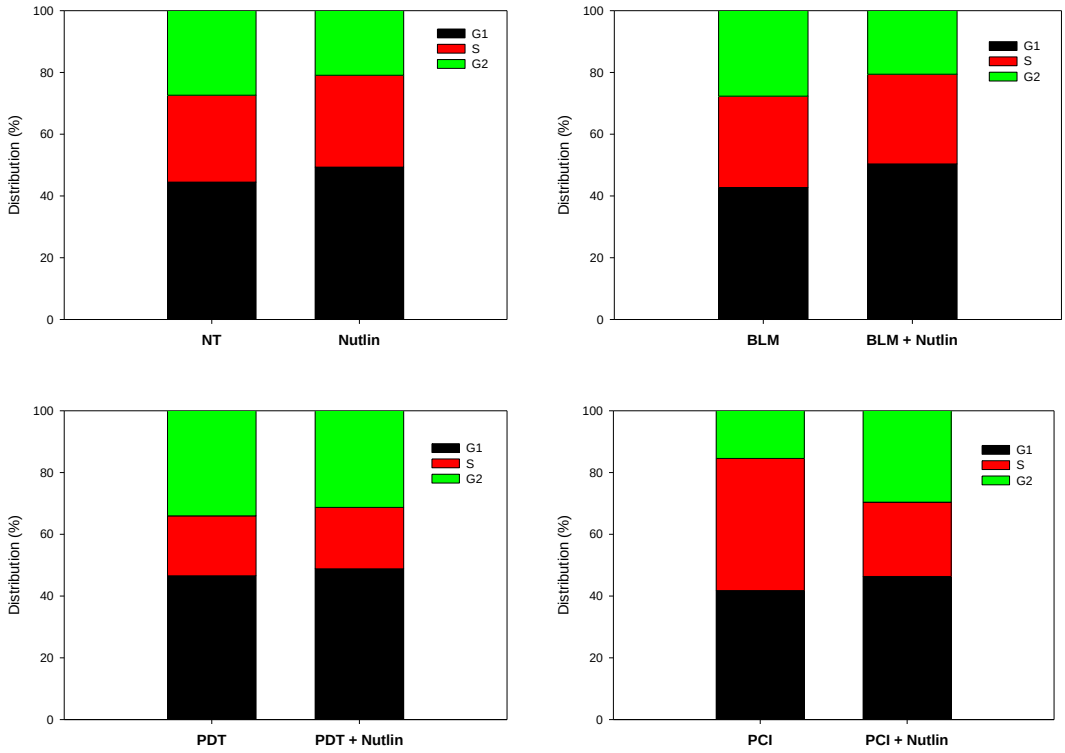

Figure 3.13: Cell cycle phase distribution 20 hours post light in SJSA-1 cells who received no treatment **(A),** 0,1 IU/ml bleomycin **(B)**, PDT **(C)** or PCI with 0,1 IU/ml bleomycin **(D)** with or without 500 nM Nutlin-3. All figures show a representative result from a single experiment.

4 Discussion

4.1 Background

The tumour suppressor p53 plays an essential role in protecting the cell from malignant transformations by inducing cell cycle arrest and apoptosis. In response to stress, a decrease in MDM2 protein levels and/or its activity and the interaction between MDM2 and p53 leads to p53 stabilisation and subsequently activation of the p53 pathway [9]. This reduction of MDM2 is crucial for p53 to exert its tumour suppressor activity.

With approximately 50% of all human malignancies containing mutations in the p53 gene [6], restoration of the p53 pathway is an attractive target for improving cancer therapy. There are several strategies for reactivating p53 in cancer cells, including adenovirus vector-mediated p53 transduction, p53 activation by regulatory proteins that modify p53, and reactivation of mutant p53. A strategy of activating wild-type p53 in $MDM2^{Ampl}$ cells targets the interaction between p53 and its negative regulator MDM2 [68]. In this study, the latter approach was investigated through the small molecule inhibitor of the MDM2-p53 interaction, Nutlin-3.

4.2 Nutlin-3

Nutlin-3 inhibits the MDM2-p53 interaction by displacing p53 from its complex with MDM2, thereby restoring the p53 pathway in vitro and in vivo [2]. Because of this direct inhibitory effect, Nutlin-3 can fully compensate for defects in the upstream p53 signalling. This requires intact downstream signalling, and it is therefore important to know of any aberrations in the p53 pathway, and to identify the tumours carrying them [69]. Nutlin-3 has been shown to be effective against a variety of cancer cells with wild-type p53, including neuroblastoma, retinoblastoma, osteosarcoma and leukemia [33]. In $p53^{Mut}$ and $p53^{Null}$ cell lines, Nutlin-3 has not shown any effect on growth and viability, suggesting that its activity is solely derived from activation of $p53^{Wt}$ signalling [1, 13]. In several tumour cell lines an increase in p21 mediated cell cycle arrest were seen upon p53 activation, but only a marginal increase in apoptosis, indicating that defective apoptotic signalling is not infrequent in solid tumours [35]. Activation of the p53 pathway with Nutlin-3 is a promising approach in cancer therapy, but further studies are needed to investigate its full therapeutic potential.

4.3 Cell lines

As a model for $p53^{Wt}$ and $MDM2^{Ampl}$ cells, the osteosarcoma cell line SJSA-1 was chosen [70]. This cell line has already been subject to extensive research on the effects of Nutlin-3 treatment, both as monotherapy and in combination with established cancer therapies [1, 35, 71-73]. The cell line SJSA-1 was used as a model for cancer cells retaining wild-type p53, but have non-functional p53 due to overexpression of MDM2. The hypothesis is that this cell line will respond well to treatment with Nutlin-3.

In addition to the SJSA-1 cell line, two other cell lines were used in this study. The leiomyosarcoma cell line SK-LMS1 express $p53^{Mut}$ and low levels of MDM2 [70]. Studies have shown little or no effect on cell cycle arrest and apoptosis of Nutlin-3 in cell lines with mutant p53, and SK-LMS1 was therefore chosen as a negative control. The third cell line included in this study was the uterine sarcoma cell line MES-SA. MES-SA express $p53^{Wt}$ and unknown levels of MDM2 [74].

4.4 Effect of Nutlin-3 on cell survival

The response to PDT and PCI treatment with saporin and bleomycin was investigated in SK-LMS1, MES-SA and SJSA-1 cells (figure 3.3-3.5). All cell lines responded well to treatment, and a greater loss of viability was seen after PCI treatment compared to PDT. These experiments were only done once, and should be repeated to confirm and possibly quantify the differences.

To investigate the effect Nutlin-3 treatment has on cell survival after PDT and PCI treatment, the same experiments was carried out in the SJSA-1 cell line with half the cells being treated with 500 nM Nutlin-3. In the cells treated with PCI of saporin there were very small differences in loss of viability between the SJSA-1 cells that were incubated with Nutlin-3 and those that were not (figure 3.7B-D). In the PDT treated cells (figure 3.7A) there appears to be an increased loss of viability in the Nutlin-3 treated cells, and this difference is more distinct than for the PCI treated cells. After PCI of bleomycin in SJSA-1 cells, only a slight difference in loss of viability is seen between the cells treated with Nutlin-3 and those only receiving PCI treatment, as measured by the clonogenic assay (figure 3.8B). It appears to be a greater difference in the PDT treated cells (figure 3.8A), but this difference is smaller than for PDT in the presence or absence of Nutlin-3 when measured by the MTT assay 48 hours post light (figure 3.7A).

In 2012, Wang *et al.* studied the effect of Nutlin-3 on cell viability of the $p53^{Wt}$ osteosarcoma cell line U-2 OS. Nutlin-3 inhibited cell growth in a time- and dose-dependent manner, with concentrations of 2-10 μM inducing a gradual effect on cell growth [2]. In this thesis, a concentration of 0,5 μM Nutlin-3 was utilised in all experiments with the SJSA-1 cell line. This concentration did induce p21 expression (figure 3.11) thus having an impact on cell cycle progression, but it may not have been sufficient to induce significant effects on colony formation. Cell cycle arrest may affect the result of the MTT assay, but a mere delay in cell cycle progression does not necessarily reduce the clonogenicity of the cells and may therefore not give visible impact on viability when measured with the clonogenic assay. This might explain the above-mentioned difference in viability measured by MTT (figure 3.7A) and the clonogenic assay (figure 3.8A) after PDT.

4.5 Effect of Nutlin-3 on protein expression

To investigate the effect treatment with Nutlin-3 had on expression of p53 and p53 target genes, protein expression was measured with western blotting. The $p53^{Wt}$ $MDM2^{Ampl}$ cell line SJSA-1 was chosen for these experiments, and the aim was to compare the levels of p53, MDM2, p21 and Bax in the cells after PDT, PCI treatment, bleomycin treatment or no treatment with or without Nutlin-3. The experiment was done only once, so the results should be considered indicative.

The protein analysis included only those cells still attached to the surface of the wells at the time of harvest. In several of the wells, in particular those receiving PDT and PCI treatment, a large number of cells were detached from the surface and were dispersed in the medium. The medium was aspirated off prior to cell lysis, and these cells were therefore not included in the sample preparation. This may have affected the result of the measurement of the protein expression, and for future experiments, the cells dispersed in the medium should be included in the analysis.

4.5.1 Effect on p53 expression

The effect of Nutlin-3 on p53 protein expression has been studied in several different cell lines. Ohnstad *et al.* [1] showed elevated levels of p53 in the $p53^{Wt}$ cell lines SJSA-1, T778 and U2OS after treatment with the IC_{50} dose of Nutlin-3 for 24 hours compared to the control. The largest difference was seen in the $MDM2^{Ampl}$ cell lines SJSA-1 and T778. The

$p53^{Mut}$ cell line RMS13 and the $p53^{Null}$ cell line SaOS-2 did not respond to treatment with Nutlin-3.

In this study, all treatments triggered an increase in p53 expression (figure 3.9). Ohnstad *et al.* reported higher expression of p53 in SJSA-1 cells treated with Nutlin-3, and that the cells receiving treatment with Nutlin-3 in combination with cisplatin had the highest expression of p53, indicating an additive effect. The same additive effect was seen in this study. In general, the cells treated with Nutlin-3 expressed more p53 than the cells that were not treated with Nutlin-3. The cells receiving only Nutlin-3 treatment expressed more p53 than the controls, indicating that Nutlin-3 alone can induce p53 expression. The difference increased with number of hours the cells were incubated with Nutlin-3, showing that the number of hours the cells are treated with Nutlin-3 has an impact on p53 expression. This is consistent with publications reporting a time-dependent activation of p53 by Nutlin-3 [75, 76].

The expression of p53 is highest 8 hours and 48 hours post light, which is consistent with results previously reported by Tovar *et al.* [35]. The rise in p53 level 8 hours post light may originate in the PDT effect, while the second rise may be due to the effect of bleomycin. Bleomycin is a slow acting substance, and may therefore require more time to induce an increase in the p53 expression. After 48 hours the p53 expression in the cells treated with bleomycin with or without Nutlin-3 is considerably higher than at 8 and 24 hours indicating that the rise in p53 level occurs later after treatment with bleomycin than after PDT and PCI treatment.

The PCI treated cells express more p53 than the other cells 8 to 48 hours post light. The difference is most distinct after 8 hours and this may be due to both the PDT effects and the effects of the bleomycin released in the cytosol upon light exposure.

4.5.2 Effect on MDM2 expression

MDM2 regulates p53 through an autoregulatory feedback loop in which both proteins mutually control their cellular level. Increased levels of p53 activate *mdm2* gene transcription, leading to elevated levels of MDM2. In turn, MDM2 binds to p53 and negatively regulates its stability and activity. This feedback loop keeps p53 under tight control and prevents it from inducing cell cycle arrest and apoptosis in normal proliferating cells [12].

When the interaction between p53 and MDM2 is inhibited by Nutlin-3, p53 is relieved from the negative control and the cellular level of p53 may rise. The increase in p53 will subsequently activate MDM2 expression, leading to accumulation of MDM2 protein [12]. Vassilev *et al.* showed in 2004 that the level of p53, MDM2 and p21 in the $p53^{Wt}$ cell line HCT116 increased in a dose-dependent matter after treatment with Nutlin. In contrast, the $p53^{Mut}$ cell line SW480 showed high basal levels of p53, but no detectable MDM2 or p21 [13].

In this study, the expression of MDM2 was measured in the SJSA-1 cell line 8, 24 and 48 hours post light (figure 3.10). The level of MDM2 appears to be highest 24 hours post light. This increase might be a result of the increase in p53 8 hours post light (figure 3.9). The treatment resulting in the highest MDM2 level is bleomycin treatment. PCI treatment induced MDM2 expression more than PDT and the difference was most distinct 24 hours post light. For cells receiving bleomycin treatment, the Nutlin-3 treated cells expressed less MDM2 than the cells receiving bleomycin alone. This difference is most distinct for the cells harvested after 8 hours, while after 48 hours the difference is diminutive. We would expect higher levels in the Nutlin-3 treated cells since these cells expressed more p53 than the cells treated with bleomycin alone. In both PDT and PCI treated cells, Nutlin-3 treatment resulted in an increase in MDM2 expression. This correlates with the higher levels of p53 measured in the cells receiving Nutlin-3 treatment in addition to PDT and PCI treatment.

The measured expression of MDM2 was lower than in the control for many of the samples, and this does not match the results seen in a number of publications [1, 33, 35, 77]. In addition, Ohnstad *et al.* reported that Nutlin-3 treatment significantly induced MDM2 expression in SJSA-1 compared to control, which does not correlate with the results in this study. The experiment should therefore be repeated to confirm or refute the results in this study.

4.5.3 Effect on p21 expression

With its ability to induce cell cycle arrest, p21 is an important protein in the cells response to DNA damage [18]. Increased levels of p53 can activate the transcription of the cyclin-dependent kinase inhibitor p21, thereby blocking cell cycle progression and if deemed necessary induce apoptosis [78]. Measuring the expression of p21 is therefore a useful tool to study the effect of Nutlin-3 treatment.

Ohnstad *et al.* [1] studied the expression of p21 in 5 different cell lines after treatment with Nutlin-3. In the $p53^{Wt}$ cell lines SJSA-1, T778 and U2OS the level of p21 was elevated in the cells receiving Nutlin-3 treatment compared to control. The difference was particularly profound in the $MDM2^{Ampl}$ cell line SJSA-1. In the $p53^{Mut}$ cell lines, there was no apparent difference in the p21 expression in the Nutlin-3 treated cells and the controls.

The results from this study indicate that the expression of p21 is considerably higher in the cells receiving Nutlin-3 treatment (figure 3.11). This is a good indicator that Nutlin-3 inhibits the p53-MDM2 interaction, thus allowing a raise in the p53 level with subsequent transcription of p21. The p21 level is higher 8 hours post light than 24 and 48 hours post light, indicating that the transcription of p21 is initiated $\leq$ 8 hours post light. This is consistent with the results of Ahmad *et al.* reporting that PDT significantly induced p21 expression 3, 6 and 12 hours after treatment [79]. The expression of p21 is higher in the cells receiving PCI treatment than for any of the other treatments, especially 8 hours post light. This correlates with the expression of p53 (figure 3.9), which is higher in the PCI treated cells, indicating that PCI strongly activates the p53 pathway. The expression of p21 is higher in PDT treated cells than bleomycin treated cells 8 and 24 hours post light, while 48 hours post light the opposite is seen. These results also correlate with the expression of p53, which follows the same pattern.

4.5.4 Effect on Bax expression

The Bcl-2 family protein Bax is one of the main regulators of the mitochondrial pathway of apoptosis. Once activated, Bax will act as a direct activator of the apoptotic pore in the mitochondria, leading to cytochrome c release and controlled cell death [80]. Bax is a downstream p53 target, and an activation of p53 will potentially lead to increase in Bax. Studying the expression of Bax is therefore of great value when investigating the effect Nutlin-3 has on the induction of apoptosis.

Miyachi *et al.* reported in 2009 that Nutlin-3 treatment increased the mRNA levels of Bax by 1.3-fold to 2.5-fold in the three $p53^{Wt}$ cell lines RMS-YM, Rh18 and RM2. In contrast, Nutlin-3 induced only a slight difference in the mRNA levels of Bax in Rh30 and RD cell lines with mutant p53 [33]. In 2012, Mochizuki *et al.* studied the effect of Nutlin-3 on Bax expression and apoptosis. They reported a significant increase of Bax mRNA in the three $p53^{Wt}$ feline lymphoma cell lines FT-1, FTG and MS4 upon Nutlin treatment that was not seen in the $p53^{Mut}$ cell lines 3201 and MCC. These results were supported by a dose-

dependent induction of apoptosis in the $p53^{Wt}$ cells. In the $p53^{Mut}$ cells, no increase in apoptosis was observed, even after incubation Nutlin-3 concentration as high as 20 μM [68].

In this study, the cells receiving Nutlin-3 treatment in addition to PDT and PCI treatment showed an increase in Bax compared to those not treated with Nutlin-3 (figure 3.12). This correlates with the results in section 3.3.4 showing a greater loss of viability in the PDT and PCI treated cells incubated with Nutlin-3 than after PDT and PCI treatment alone. The expression of Bax is higher after PCI treatment than after PDT. This correlates with the results in section 3.3.2 where PCI of bleomycin induces a greater loss of viability than PDT. The Bax level appears to be higher 24 hours post light than 8 and 48 hours post light. As discussed above, the transcription of p21 is initiated ≤ 8 hours post light. It appears that the cells are given time to stop in the cell cycle and attempt DNA damage repair before apoptosis is eventually induced.

One great weakness to these results is that the cells not attached to the surface of the wells were not included in the analysis. Early in apoptosis the cells round up and may detach from the surface and their neighbouring cells. It is therefore reason to believe that many of the apoptotic cells, expressing high level of Bax, were lost during sample preparation. This experiment should be repeated, including the cells dispersed in the medium.

4.6 Cell cycle analysis

p21 mediated induction of cell cycle arrest in response to stress is one of the key features of p53 as a tumour suppressor. p21 binds to and inhibits the kinase activity of the cyclin-dependent kinases (CDKs) CDK_1 and CDK_2 leading to growth arrest mainly in the G_1 phase of the cell cycle [81, 82]. This growth arrest gives the cells time to repair the DNA damage, or in the event of irreparable damage, apoptosis is induced [17]. Cell cycle analysis is a valuable tool in studying the effect Nutlin-3 has on the p53 pathway.

Several studies have looked into the cell cycle effect of Nutlin-3 in different cell lines. Miyachi *et al.* reported in 2009 that a 24-hour treatment with Nutlin-3 arrested the cell cycle of rhabdomyosarcoma cells with wild-type p53, decreasing the S-phase fraction from 30-40% to 5-20%. In contrast, Nutlin-3 had no effect on the cell cycle progression of Rh30 and RD cell lines with mutated p53 [33]. In 2012, Wang *et al.* reported that Nutlin-3 induced G_1 arrest in $p53^{Wt}$ U-2 osteosarcoma cells in a dose-dependent way [83]. The study showed that treatment with 10 μM Nutlin-3 significantly increased G_1 phase and decreased S-phase

fraction in U-2 OS cells but gave no significant increase in G_1-phase fraction in $p53^{Mut}$ cell line MG63 or $p53^{Null}$ cell line SaOS2.

In this study, a cell cycle analysis of the $p53^{Wt}$ $MDM2^{Ampl}$ cell line SJSA-1 was carried out. The cells were treated with bleomycin, PDT or PCI of bleomycin with or without 0,5 μM Nutlin-3. After 20 hours (figure 3.13), the PCI cells treated with Nutlin-3 appears to have a substantial decrease in the S-phase fraction and an increase in the G_1-phase fraction. The S-phase fraction of these cells was substantially higher than measured in SJSA-1 cells treated with 10 μM Nutlin-3 by Tovar *et al.* in 2006 [35]. In this paper, Tovar *et al.* reported that Nutlin-3 induced p21 expression in a dose-dependent matter, which might explain the greater impact on cell cycle they reported. As previously seen in this study, Nutlin-3 induces expression of p21 through activation of the p53-pathway (figure 3.11). The expression of p21 8 hours post light is substantially higher in the cells treated with PCI and Nutlin-3 than for any other treatment. This may explain the great difference in S-phase fraction between PCI treated cell in the presence or absence of Nutlin-3 that is not seen in any of the other samples.

When the SJSA-1 cells were treated with PCI of bleomycin (figure 3.8), the presence and absence of Nutlin-3 had only limited impact on cell viability, as measured with the clonogenic assay. The expression of Bax after PCI of bleomycin did not show great differences in the presence or absence of Nutlin-3 (figure 3.12). The results in this study indicates that 500 nM Nutlin-3 triggers cell cycle arrest after PCI of bleomycin, but does not induce apoptosis to a great extent. When considering the dose-dependent effects of Nutlin-3 on cell cycle and cell viability reported by Wang *et al.* [83], it may be wise to optimise the Nutlin-3 dose for future experiments both regarding the concentration of Nutlin-3 added and the timing of the treatment.

5 Conclusion

In this study, the impact of Nutlin-3 on cell survival, cell cycle progression and expression of p53 and p53 downstream targets after PDT and PCI treatment was investigated. The results show that Nutlin-3 activated the p53 pathway inducing the expression of the p53 downstream targets MDM2, p21 and Bax in the $p53^{Wt}$ $MDM2^{Ampl}$ osteosarcoma cell line SJSA-1. Furthermore, the study showed that Nutlin-3 induces cell cycle arrest in the G_1/S checkpoint in SJSA-1 cells after treatment with PCI of bleomycin. The impact of Nutlin-3 on cell survival after PDT and PCI of saporin and bleomycin is still not clear, but the results indicate that Nutlin-3 does have a negative impact on cell growth. Future work on different cell lines and optimisation of Nutlin-3 doses and timing needs to be done to better evaluate the therapeutic potential of Nutlin-3.

The present study suggest that the combination of Nutlin-3 and PCI treatment could be a promising therapeutic strategy for tumours with non-functional p53 due to overexpression of MDM2.

Bibliography

1. Ohnstad, H.O., et al., *MDM2 antagonist Nutlin-3a potentiates antitumour activity of cytotoxic drugs in sarcoma cell lines.* BMC Cancer, 2011. **11**(1): p. 211.
2. Wang, W. and Y. Hu, *Small molecule agents targeting the p53-MDM2 pathway for cancer therapy.* Medicinal Research Reviews, 2012. **32**(6): p. 1159-1196.
3. Bond, G.L., W. Hu, and A.J. Levine, *MDM2 is a central node in the p53 pathway: 12 years and counting.* Curr Cancer Drug Targets, 2005. **5**(1): p. 3-8.
4. Alberts B, et al., *The Molecular Basis of Cancer-Cell Behavior*, in *Molecular Biology of the Cell*. 2002, Garland Science: New York.
5. Levine, A.J. and M. Oren, *The first 30 years of p53: growing ever more complex.* Nature Reviews Cancer, 2009. **9**(10): p. 749-758.
6. Hollstein, M., et al., *Database of p53 gene somatic mutations in human tumors and cell lines.* Nucleic acids research, 1994. **22**(17): p. 3551.
7. Levine, A.J., *p53, the Cellular Gatekeeper for Growth and Division.* Cell, 1997. **88**(3): p. 323-331.
8. Freedman, D.A., L. Wu, and A.J. Levine, *Functions of the MDM2 oncoprotein.* Cellular and Molecular Life Sciences CMLS, 1999. **55**(1): p. 96-107.
9. Marine, J.-C. and G. Lozano, *Mdm2-mediated ubiquitylation: p53 and beyond.* Cell Death & Differentiation, 2009. **17**(1): p. 93-102.
10. Shieh, S.-Y., et al., *DNA Damage-Induced Phosphorylation of p53 Alleviates Inhibition by MDM2.* Cell, 1997. **91**(3): p. 325-334.
11. Vassilev, L.T., *MDM2 inhibitors for cancer therapy.* Trends in Molecular Medicine, 2007. **13**(1): p. 23-31.
12. Vassilev, L.T., *p53 Activation by Small Molecules: Application in Oncology.* Journal of Medicinal Chemistry, 2005. **48**(14): p. 4491-4499.
13. Vassilev, L.T., et al., *In Vivo Activation of the p53 Pathway by Small-Molecule Antagonists of MDM2.* Science, 2004. **303**(5659): p. 844-848.
14. Alberts B, et al., *The Cell Cycle and Programmed Cell Death*, in *Molecular Biology of the Cell*. 2002, Garland Science: New York.
15. Alberts B, et al., *An Overview of the Cell Cycle*, in *Molecular Biology of the Cell*. 2002, Garland Science: New York.
16. Alberts B, et al., *Components of the Cell-Cycle Control System*, in *Molecular Biology of the Cell*. 2002, Garland Science New York.
17. Yoshida, K. and Y. Miki, *The cell death machinery governed by the p53 tumor suppressor in response to DNA damage.* Cancer Science, 2010. **101**(4): p. 831-835.
18. Bartek, J. and J. Lukas, *Pathways governing G1/S transition and their response to DNA damage.* FEBS Letters, 2001. **490**(3): p. 117-122.
19. *The Cell Cycle*. 2013 Accessed 06-05-2013]; Available from: http://moodleshare.org/mod/book/view.php?id=2115&chapterid=261.
20. Mirzayans, R., et al., *New Insights into p53 Signaling and Cancer Cell Response to DNA Damage: Implications for Cancer Therapy.* Journal of Biomedicine and Biotechnology, 2012. **2012**: p. 16.
21. Ljungman, M., *Dial 9-1-1 for p53: mechanisms of p53 activation by cellular stress.* Neoplasia (New York, NY), 2000. **2**(3): p. 208.
22. Harris, S.L. and A.J. Levine, *The p53 pathway: positive and negative feedback loops.* Oncogene, 2005. **24**(17): p. 2899-2908.

23. Jeggo, P.A. and M. Löbrich, *Contribution of DNA repair and cell cycle checkpoint arrest to the maintenance of genomic stability.* DNA Repair, 2006. **5**(9–10): p. 1192-1198.
24. Haupt, S., et al., *Apoptosis - the p53 network.* Journal of Cell Science, 2003. **116**(20): p. 4077-4085.
25. Ozaki, T. and A. Nakagawara, *p53: The Attractive Tumor Suppressor in the Cancer Research Field.* Journal of Biomedicine and Biotechnology, 2011. **2011**.
26. Bellini, M.F., et al., *Alterations of the TP53 Gene in Gastric and Esophageal Carcinogenesis.* Journal of Biomedicine and Biotechnology, 2012. **2012**.
27. Matsumura, Y. and H.N. Ananthaswamy, *The central role of p53 in cell-cycle arrest, DNA repair and apoptosis following UV irradiation.* Expert Reviews in Molecular Medicine, 2002.
28. Shangary, S. and S. Wang, *Small-molecule inhibitors of the MDM2-p53 protein-protein interaction to reactivate p53 function: a novel approach for cancer therapy.* Annual review of pharmacology and toxicology, 2009. **49**: p. 223-241.
29. Pan, D., et al., *Stabilisation of p53 enhances reovirus-induced apoptosis and virus spread through p53-dependent NF-[kappa]B activation.* Br J Cancer, 2011. **105**(7): p. 1012-1022.
30. Pishas, K.I., et al., *Nutlin-3a Is a Potential Therapeutic for Ewing Sarcoma.* Clinical Cancer Research, 2011. **17**(3): p. 494-504.
31. Coll-Mulet, L., et al., *MDM2 antagonists activate p53 and synergize with genotoxic drugs in B-cell chronic lymphocytic leukemia cells.* Blood, 2006. **107**(10): p. 4109-4114.
32. Drakos, E., et al., *Inhibition of p53-Murine Double Minute 2 Interaction by Nutlin-3A Stabilizes p53 and Induces Cell Cycle Arrest and Apoptosis in Hodgkin Lymphoma.* Clinical Cancer Research, 2007. **13**(11): p. 3380-3387.
33. Miyachi, M., et al., *Restoration of p53 Pathway by Nutlin-3 Induces Cell Cycle Arrest and Apoptosis in Human Rhabdomyosarcoma Cells.* Clinical Cancer Research, 2009. **15**(12): p. 4077-4084.
34. Gu, L., et al., *MDM2 antagonist nutlin-3 is a potent inducer of apoptosis in pediatric acute lymphoblastic leukemia cells with wild-type p53 and overexpression of MDM2.* Leukemia, 2008. **22**(4): p. 730-739.
35. Tovar, C., et al., *Small-molecule MDM2 antagonists reveal aberrant p53 signaling in cancer: Implications for therapy.* PNAS, 2006. **103**(6): p. 1888-1893.
36. Ackroyd, R., et al., *The History of Photodetection and Photodynamic Therapy.* Photochemistry and Photobiology, 2001. **74**(5): p. 656-669.
37. Lipson Rl, B.E., *The photodynamic properties of a particular hematoporphyrin derivative.* Archives of Dermatology, 1960. **82**(4): p. 508-516.
38. Diamond, I., et al., *Photodynamic Therapy of Malignant Tumours.* The Lancet, 1972. **300**(7788): p. 1175-1177.
39. Dougherty, T.J., et al., *Photoradiation Therapy. II. Cure of Animal Tumors With Hematoporphyrin and Light.* Journal of the National Cancer Institute, 1975. **55**(1): p. 115-121.
40. Agostinis, P., et al., *Photodynamic therapy of cancer: An update.* CA: A Cancer Journal for Clinicians, 2011. **61**(4): p. 250-281.
41. Macdonald, I.J. and T.J. Dougherty, *Basic principles of photodynamic therapy.* Journal of Porphyrins and Phthalocyanines, 2001. **5**(2): p. 105-129.
42. Dolmans, D.E.J.G.J., D. Fukumura, and R.K. Jain, *Photodynamic therapy for cancer.* Nat Rev Cancer, 2003. **3**(5): p. 380-387.

43. Moan, J. and K. Berg, *The photodegradation of porphyrins in cells can be used to estimate the lifetime of singlet oxygen* Photochemistry and Photobiology, 1991. **53**(4): p. 549-553.
44. Huang, Z., *A review of progress in clinical photodynamic therapy.* Technology in cancer research & treatment, 2005. **4**(3): p. 283.
45. Berg, K., et al., *Photochemical internalization (PCI): A novel technology for activation of endocytosed therapeutic agents.* Medical Laser Application, 2006. **21**(4): p. 239-250.
46. Norum, O.-J., et al., *Photochemical internalization (PCI) in cancer therapy: From bench towards bedside medicine.* Journal of Photochemistry and Photobiology B: Biology, 2009. **96**(2): p. 83-92.
47. Selbo, P.K., et al., *Photochemical internalization provides time- and space-controlled endolysosomal escape of therapeutic molecules.* Journal of Controlled Release, 2010. **148**(1): p. 2-12.
48. Belting, M., S. Sandgren, and A. Wittrup, *Nuclear delivery of macromolecules: barriers and carriers.* Advanced Drug Delivery Reviews, 2005. **57**(4): p. 505-527.
49. Berg, K., et al., *Photochemical Internalization: A Novel Technology for Delivery of Macromolecules into Cytosol.* Cancer Research, 1999. **59**(6): p. 1180-1183.
50. Berg, K., et al., *Disulfonated tetraphenyl chlorin (TPCS2a), a novel photosensitizer developed for clinical utilization of photochemical internalization.* Photochem Photobiol Sci, 2011. **10**(10): p. 1637-51.
51. Høgset, A., et al., *Photochemical internalisation in drug and gene delivery.* Advanced Drug Delivery Reviews, 2004. **56**(1): p. 95-115.
52. Weyergang, A., et al., *Photochemical internalization of tumor-targeted protein toxins.* Lasers Surg Med, 2011. **43**(7): p. 721-33.
53. *LumiSource - novel light source for 'in vitro' research*. [cited 2013 6 March]; Available from: http://www.pcibiotech.no/content/lumisource-novel-light-source-vitro-research.
54. van Meerloo, J., G.J. Kaspers, and J. Cloos, *Cell sensitivity assays: the MTT assay.* Methods Mol Biol, 2011. **731**: p. 237-45.
55. Sylvester, P.W., *Optimization of the Tetrazolium Dye (MTT) Colorimetric Assay for Cellular Growth and Viability*, in *Drug Design and Discovery*, S.D. Satyanarayanajois, Editor. 2011, Humana Press. p. 157-168.
56. Sumantran, V.N., *Cellular chemosensitivity assays: an overview.* Methods Mol Biol, 2011. **731**: p. 219-36.
57. Franken, N.A., et al., *Clonogenic assay of cells in vitro.* Nat Protoc, 2006. **1**(5): p. 2315-9.
58. Osborne, C. and S.A. Brooks, *SDS-PAGE and Western Blotting to Detect Proteins and Glycoproteins of Interest in Breast Cancer Research*, in *Breast Cancer Researh Protocols*, S. Brooks and A. Harris, Editors. 2006, Humana Press. p. 217-229.
59. Bjerrum, O.J. and N.H.H. Heegaard, *Western Blotting: Immunoblotting*, in *Encyclopedia of Life Sciences* 2009, John Wiley & Sons, Ltd.
60. Kurien, B.T. and R.H. Scofield, *Western blotting.* Methods, 2006. **38**(4): p. 283-93.
61. *General Western Blot Protocol*. Accessed 06-05-2013]; Available from: http://www.leinco.com/general_wb.
62. Dean, P.N. and R.A. Hoffman, *Overview of Flow Cytometry Instrumentation*, in *Current Protocols in Cytometry*. 2001, John Wiley & Sons, Inc.
63. Darzynkiewicz, Z., et al., *Cytometry in cell necrobiology: Analysis of apoptosis and accidental cell death (necrosis).* Cytometry, 1997. **27**(1): p. 1-20.

64. Brown, M. and C. Wittwer, *Flow Cytometry: Principles and Clinical Applications in Hematology.* Clinical Chemistry, 2000. **46**: p. 1221-1229.
65. Heatwole, V.M., *TUNEL Assay for Apoptotic Cells*, in *Immunocytochemical Methods and Protocols*, L. Javois, Editor. 1999, Humana Press. p. 141-148.
66. Kuo, L.J. and L.-X. Yang, *γ-H2AX - A Novel Biomarker for DNA Double-strand Breaks.* In Vivo, 2008. **22**: p. 305-309.
67. Chasin, L. and D. Mowshowitz. *Exponential Growth*. 2000 Accessed 03-05-2013]; Available from: http://ccnmtl.columbia.edu/projects/biology/lecture1/expogrow.html.
68. Mochizuki, H., et al., *Comparison of the antitumor effects of an MDM2 inhibitor, nutlin-3, in feline lymphoma cell lines with or without p53 mutation.* Veterinary Immunology and Immunopathology, 2012. **147**(3–4): p. 187-194.
69. Vu, B.T. and L. Vassilev, *Small-Molecule Inhibitors of the p53-MDM2 Interaction.* Current Topics in Microbiology and Immunology, 2011. **348**: p. 151-172.
70. Lin, J., et al., *A modified p53 overcomes mdm2-mediated oncogenic transformation: a potential cancer therapeutic agent.* Cancer research, 2000. **60**(20): p. 5895-5901.
71. Du, W., et al., *Nutlin-3 Affects Expression and Function of Retinoblastoma Protein: Role of Retinoblastoma Protein in Cellular Response to Nutlin-3.* Journal of Biological Chemistry, 2009. **284**(39): p. 26315-26321.
72. Carvajal, D., et al., *Activation of p53 by MDM2 Antagonists Can Protect Proliferating Cells from Mitotic Inhibitors.* Cancer Research, 2005. **65**(5): p. 1918-1924.
73. Müller, C.R., et al., *Potential for treatment of liposarcomas with the MDM2 antagonist Nutlin-3A.* International Journal of Cancer, 2007. **121**(1): p. 199-205.
74. Zhu, Q.-S., et al., *Soft Tissue Sarcoma Cells Are Highly Sensitive to AKT Blockade: A Role for p53-Independent Up-regulation of GADD45α.* Cancer Research, 2008. **68**(8): p. 2895-2903.
75. Valentine, J., S. Kumar, and A. Moumen, *A p53-independent role for the MDM2 antagonist Nutlin-3 in DNA damage response initiation.* BMC Cancer, 2011. **11**(1): p. 1-11.
76. Supiot, S., R.P. Hill, and R.G. Bristow, *Nutlin-3 radiosensitizes hypoxic prostate cancer cells independent of p53.* Molecular Cancer Therapeutics, 2008. **7**(4): p. 993-999.
77. Sonnemann, J., et al., *Anticancer effects of the p53 activator nutlin-3 in Ewing's sarcoma cells.* European journal of cancer (Oxford, England : 1990), 2011. **47**(9): p. 1432-1441.
78. Vousden, K.H. and C. Prives, *Blinded by the Light: The Growing Complexity of p53.* Cell, 2009. **137**(3): p. 413-431.
79. Ahmad, N., et al., *Photodynamic therapy results in induction of WAF1/CIP1/P21 leading to cell cycle arrest and apoptosis.* Proceedings of the National Academy of Sciences, 1998. **95**(12): p. 6977-6982.
80. Basañez, G., L. Soane, and J.M. Hardwick, *A New View of the Lethal Apoptotic Pore.* PLoS Biol, 2012. **10**(9): p. e1001399.
81. Abbas, T. and A. Dutta, *p21 in cancer: intricate networks and multiple activities.* Nat Rev Cancer, 2009. **9**(6): p. 400-414.
82. Sullivan, K.D., et al., *The p53 circuit board.* Biochimica et Biophysica Acta (BBA) - Reviews on Cancer, 2012. **1825**(2): p. 229-244.
83. Wang, B., et al., *MDM2 inhibitor Nutlin-3a suppresses proliferation and promotes apoptosis in osteosarcoma cells.* Acta Biochimica et Biophysica Sinica, 2012. **44**(8): p. 685-691.

Appendix A

Lysis buffer for SDS-PAGE

10 µl NaF 200 mM in dH_2O

10 µl PMSF 200 nM in isopropanol

10 µl activated Na_2VO_4

20 µl β-glycerol phosphate 2 M in dH_2O

20 µl phosphatase inhibitor cocktail I (Sigma-Aldrich)

20 µl phosphatase inhibitor cocktail II (Sigma-Aldrich)

20 µl protease inhibitor cocktail (Sigma-Aldrich)

Ad 2 ml sample buffer

Sample buffer

6,2 mM Tris-HCl

2% (w/v) SDS (Bio-Rad)

10% (w/v) glycerol (VWR)

50 mM DTT (Sigma-Aldrich)

0,01% bromphenol blue

Transfer buffer

3,75 g SDS

15,1 g Trizma® Base

71,4 g glycine

1 L methanol (VWR)

Ad 5 L dH_2O

10 x Running buffer pH 8,3

10 g SDS

30 g Trizma® Base (Sigma-Aldrich)

144 g glycine (Sigma-Aldrich)

Ad 1 L dH_2O

1 x Running buffer

100 ml 10x Running buffer

Ad 1 L dH_2O

10 x TBS pH 7,6

12,11 g Trizma® Base

87,66 g NaCl

Ad 1 L dH_2O

1 x TTBS

100 ml 10x TBS

100 ml Tween 20 (Sigma-Aldrich)

Ad 1 L dH_2O

Separating gel with 12% acrylamide (1 gel)

2,45 ml ddH_2O

1,9 ml 1,5M Tris-HCl pH 8,8

75 µl 10% (w/v) SDS

0,75 ml glycerol

2,25 ml 40% Acrylamide/Bis solution (Bio-Rad)

75 µl 10% ammonium persulfate (Bio-Rad)

5 µl TEMED

Stacking gel (1 gel)

3,2 ml ddH_2O

1,25 ml 0,5M Tris-HCl pH 6,8

50 µl 10% SDS

0,5 ml 40% Acrylamide/Bis solution

25 µl 10% ammonium persulfate

5 µl TEMED

10% sodium dodecyl sulfate (SDS)

10 g SDS

Ad 100 ml dH_2O

0,5M Tris-HCl pH 6,8

17,5 g Tris-HCl

1,7 g Trizma® Base

dH_2O ad 250 ml

0,5M Tris-HCl pH 8,8

9,23 g Tris-HCl

38,5 g Trizma® Base

dH_2O ad 250 ml

5% non-fat dry milk solution

5 g skimmed milk powder

100 ml TTBS

5% BSA solution

5 g BSA (Sigma-Aldrich)

100 ml TTBS

TdT reaction solution (6 samples)

0,96 µl TdT enzyme (Roche Applied Science, Indianapolis, IN, USA)

24 µl TdT reaction buffer (Roche Applied Science)

14,4 µl $CoCl_2$ (25 mM) (Roche Applied Science)

2,4 µl Biotin-16-dUTP (Roche Applied Science)

2,4 µl DTT (10 mM) (Sigma-Aldrich)

196 µl ddH_2O

10 mM DTT

15,425 mg Dithiothreiol (MW = 154,25 g/mol) (Sigma-Aldrich)

10 ml dH_2O

Primary Ab for Flow Cytometry (6 samples)

0,67 µl mouse α-γH2AX (Millipore)

0,67 µl rabbit α-P-histone-H3 (Millipore)

332 µl 5% non-fat dry milk in PBS

Secondary Ab for Flow Cytometry (6 samples)

6,67 µl goat α-rabbit-PE (Invitrogen/Life Technologies, Carlsbad, CA, USA)

6,67 µl rabbit α-mouse-FITC (Dako, Glostrup, Denmark)

0,83 µl Streptavidin-Cy5 (GE Healthcare)

319,17 µl 5% non-fat dry milk in PBS

Appendix B

Ladder for SDS-PAGE

Substance:	Produced by:	Diluted in:	Dilution:	2• antibody:
Kaleidoskop	Bio Rad	Lysis buffer	2:5	None
Biotinylated ladder	Cell Signaling	Lysis Buffer	1:5	Anti-Biotin

Primary antibodies used for immune detection in Western blotting

1• antibody:	Produced by:	Diluted in:	Dilution:	2• antibody:
Anti-p53 (sc-6243)	Santa Cruz	5 % milk	1:1000	Anti-rabbit
Anti-p21 (sc-397)	Santa Cruz	5 % milk	1:1000	Anti-rabbit
Anti-MDM2 (ab38168)	AbCam	5 % BSA	1:300	Anti-rabbit
Anti-Bax (#2772)	Cell Signaling	5 % BSA	1:1000	Anti-rabbit

Secondary antibodies used for immune detection in Western blotting

2• antibody:	Produced by:	Diluted in:	Dilution:
Anti-biotin (#7075)	Cell Signaling	5 % milk	1:1000
Anti-rabbit (#7074S)	Cell Signaling	5 % milk	1:5000